An Efficient Homotopy Method for Solving the Post-contingency Optimal Power Flow to Global Optimality*

SangWoo Park
Department of Industrial Engineering and Operations Research, University of California, Berkeley, spark111@berkeley.edu

Elizabeth Glista
Department of Mechanical Engineering, University of California, Berkeley, glista@berkeley.edu

Javad Lavaei
Department of Industrial Engineering and Operations Research, University of California, Berkeley, lavaei@berkeley.edu

Somayeh Sojoudi
Department of Electrical Engineering and Computer Sciences, University of California, Berkeley, sojoudi@berkeley.edu

Optimal power flow (OPF) is a fundamental problem in power systems analysis for determining the steady-state operating point of a power network that minimizes the generation cost. In anticipation of component failures, such as transmission line or generator outages, it is also important to find optimal corrective actions for the power flow distribution over the network. The problem of finding these post-contingency solutions to the OPF problem is challenging due to the nonconvexity of the power flow equations and the large number of contingency cases in practice. In this paper, we introduce a homotopy method to solve for the post-contingency actions, which involves a series of intermediate optimization problems that gradually transform the original OPF problem into each contingency-OPF problem. We show that given a global solution to the original OPF problem, a global solution to the contingency problem can be obtained using this homotopy method, under some conditions. With simulations on Polish and other European networks, we demonstrate that the effectiveness of the proposed homotopy method is dependent on the choice of the homotopy path and that homotopy yields an improved solution in many cases.

Key words: Power systems, optimal power flow, nonconvex optimization, contingency analysis

1. Introduction

Optimal power flow (OPF) is a fundamental tool for power system network analysis, where the goal is to find a low-cost production of the committed generating units while satisfying the technical constraints of the system [2]. The main challenges in solving the OPF arise from the fact that it is a nonconvex optimization problem on a large-scale network that must be solved every few minutes. In order to overcome these challenges, the common practice in the electric power industry is to use a linearized approach called the DC-OPF approximation [3, 4], as opposed to the original AC-OPF

problem. However, such methods simplify important aspects of the power flow physics and cannot guarantee attaining any optimal solution of the original problem. Improvements in interior-point methods have also provided an effective tool for solving the OPF problem, but they only guarantee convergence to a locally optimal solution [5, 6, 7]. Despite its difficulty, finding a global optimum for a large-scale OPF problem modeled with AC power flow equations is crucial for the reliable and efficient operation of power systems.

Initiated by the work [8], conic optimization has been extensively studied in recent years and proven to be a powerful technique for solving OPF to global or near-global optimality. The paper [8] has indeed shown that a semidefinite programming (SDP) relaxation is able to find a global minimum of OPF for a large class of practical systems, and [9] has discovered that the success of this method is related to the underlying physics of power systems. [10] and [11] have developed different sufficient conditions under which the SDP relaxation provides zero duality gap. Moreover, [12] has found an upper bound on the the rank of the minimum-rank solution of the SDP relaxation, which is leveraged in [13] to find a near globally optimal solution of OPF via a penalized SDP technique in the case where the SDP relaxation fails to work. These ideas have been refined in many papers to improve the relaxations via branch-and-cut approaches, conic hierarchies, and valid inequalities [14, 15, 16, 17]. In order to tackle the computational burden of solving large-scale SDP relaxations, the authors of [18] proposed strong second-order cone programming (SOCP) relaxations, which produce high-quality feasible solutions for the AC-OPF problem in a short amount of time. The reader is referred to the survey paper [19] for more details.

Recently, there has been elevated interest in studying the robust operations of power systems that can withstand element failures (contingencies) in the network. Power operators are required to solve the *security-constrained* OPF (SCOPF) instead of an idealistic OPF problem [20, 21]. SCOPF is formulated by adding extra constraints to the classic OPF discussed above. These constraints impose additional limits on line flows and nodal voltages for a predetermined set of post-contingency configurations. In other words, SCOPF can be regarded as a more conservative version of the classic OPF that leads to a higher level of system security. This means that SCOPF inherits the challenges of classic OPF and furthermore, invites new challenges. It has been shown in [13] that SDP relaxations are able to obtain high-quality solutions of SCOPF. However, since SCOPF is a gigantic problem with an enormous number of variables, conic relaxations and even simple local search methods may be ineffective for real-world systems [22]. There are two primary methods to address the huge size of the SCOPF problem. One approach is to reduce the number of contingencies to a subset of binding contingencies that will lead to the same solution as the full set of contingencies [23, 24, 25]. If the number of binding contingencies is not sufficiently small enough to satisfy computational requirements, then we must make use of the second method, which is to

simplify the SCOPF formulation. There have been many proposed methods to simplify the model of post-contingency states in SCOPF, such as Benders decomposition, linearization of the power flow equations, Lagrangian relaxation, and network compression [26, 27, 28, 29]. These contingency selection, approximation, and decomposition techniques can be combined to generate heuristic solutions to large-scale SCOPF problems, as in [30, 31]. Additionally, recent research has applied approaches from distributed control, stochastic programming, and machine learning to solve the SCOPF problem [32, 33, 34, 35].

The outputs of such methods include the optimal (or approximately optimal) values of the pre-contingency operating variables and possibly feasible values for the post-contingency variables for each contingency. The major drawback is that the post-contingency variables are not optimized with respect to each corresponding contingency configuration to minimize the violation of the constraints in case there is no feasible operating point. Currently, there is a rather limited literature that attempts to optimize the post-contingency settings. In the classic work [21], the optimal post-contingency actions were modelled as sub-problems and explicitly included in the SCOPF formulation. In order to overcome the complexity of this two-level optimization problem, an algorithm based on Bender's decomposition was developed, for which convergence is not guaranteed for general nonconvex problems. More recently, the work in [36] proposed an approach to determine an optimal combination of preventive and corrective actions taking into the account the system dynamics, while [37] introduced a hybrid computational strategy to solve the pre-contingency and post-contingency OPF problems. To the best of our knowledge, none of the previous works have ventured into finding the global optimum of each of the post-contingency OPF problems (from here on called 'contingency-OPF'), mainly because applying a computationally burdensome algorithm (such as SDP) to each of the contingency scenarios is unrealistic.

Nevertheless, it is important to find a globally optimal solution because local solutions can be much more costly. In this paper, we develop a computationally efficient homotopy method to improve the quality of the contingency-OPF solution. Constraint violations in the case of a contingency are very expensive to deal with, and under our formulation, a global solution corresponds to the minimum violation. Instead of solving for the solution to a contingency-OPF problem directly, we generate and solve (using local search algorithms) a series of intermediate optimization problems wherein we gradually remove a set of components of the power system. We show that the effectiveness of homotopy to find a global solution of the contingency-OPF problem is dependent on the homotopy path, and therefore, we characterize desirable homotopy paths. In doing so, we prove that the contingency-OPF generically has a unique global minimum. Furthermore, we prove that the complexity of implementing such homotopy scheme is on the order of solving $O(\log(1/\epsilon))$ convex quadratic optimization problems.

The remainder of the paper is organized as follows. In Section 2, we provide a literature review on homotopy methods and explain how it relates to our approach. In Section 3, we present the formulation of the two-stage Security-constrained Optimal Power Flow that can be decomposed into the base-OPF and contingency-OPF. Next, in Section 4, we introduce the homotopy method that connects contingency-OPF to base-OPF via parametrization. In Section 5, we develop theoretical results to characterize cases when homotopy will lead to a global solution of the deformed problem. Finally, in Section 6 we implement the homotopy method on actual test cases and verify its effectiveness. The proofs and additional simulation results appear in the Appendix.

1.1. Notations

The symbol $\mathbb{R}^N$ denotes the space of N-dimensional real vectors and $(\cdot)^T$ denotes the transpose of a matrix. $\text{Re}\{\cdot\}$ and $\text{Im}\{\cdot\}$ denote the real and imaginary parts of a given scalar or matrix. The symbol $|\cdot|$ is the absolute value operator if the argument is a scalar, vector, or matrix; otherwise, it is the cardinality of a measurable set. Given a function $f(x,\cdot)$, $\nabla_x f(x,\cdot)$ and $\nabla_x^2 f(x,\cdot)$ denote the Jacobian and Hessian of f with respect to x, respectively. The symbol $\odot$ denotes the elementwise multiplication between two vectors. Let $\mathbf{1}_n$ and $\mathbf{0}_n$ denote the n-dimensional vectors of ones and zeros, respectively. Furthermore, $\mathbf{1}_n^k$ denotes an n-dimensional vector of ones except for the k-th element that is zero. The imaginary unit is denoted by $\mathbf{j} = \sqrt{-1}$. Let the power network be defined by a graph $\mathcal{G}(\mathcal{V},\mathcal{E})$, where $\mathcal{V}$ is the node set and $\mathcal{E}$ is the edge set. For notational simplicity, we assume that there is one generator at each node, but this formulation is easily generalizable to the case when there are multiple generators at each node (the case with no generator at a bus can be modeled by setting the upper and lower bounds on generation to zero). Each node $i \in \mathcal{V}$ has an associated complex voltage v_i, a fixed demand $P_i^d + \mathbf{j}Q_i^d$, and an unknown generation $p_i^g + \mathbf{j}q_i^g$, and we assume that the nodal shunt admittance is zero. The complex voltage v_i can be expressed in polar form, $v_i = |v_i|e^{\mathbf{j}\theta_i}$, where $|v_i|$ and θ_i denote the voltage magnitude and phase angle at bus i, respectively. With a slight abuse of notation, $|v|$ denotes the vector of all voltage magnitudes. In addition, we define $\theta_{ij} = \theta_i - \theta_j$. The set of neighboring nodes of node i is denoted by $\mathcal{N}(i)$. Each line connecting two nodes i and j is represented by a standard Π-model with a series admittance $y_{ij} = g_{ij} + \mathbf{j}b_{ij}$ and a shunt admittance $y_{ij}^{\text{sh}} = g_{ij}^{\text{sh}} + \mathbf{j}b_{ij}^{\text{sh}}$. Then, the nodal admittance matrix Y is defined as

$$Y_{ij} = \begin{cases} \sum_{k\in\mathcal{N}(i)} y_{ik} + \frac{1}{2}y_{ik}^{\text{sh}} & \text{for } j = i \\ -y_{ij} & \text{for } j \in \mathcal{N}(i) \\ 0 & \text{otherwise} \end{cases} \tag{1}$$

whose (i,j) element is denoted as $Y_{ij} = G_{ij} + \mathbf{j}B_{ij}$. Finally, p_{ij} and q_{ij} are the real and reactive power flows from bus i to j, respectively.

2. Homotopy for Optimization

Homotopy methods have been used to improve the convergence of optimization problems. The benefit of homotopy methods compared to other iterative methods is that homotopy methods may yield global rather than local convergence. These methods are most useful for problems where convergence to a global solution is heavily dependent on a good initial point, which can be hard to obtain. More recently, probability-one homotopy methods have been applied to solving optimization problems, such as optimal control [38, 39] and statistical learning [40]. Typically, the homotopy methods in optimization focus on parametrizing the first-order optimality conditions [41, 42] or the objective function ([43, 44]). Homotopy methods have also been applied in the field of power systems, primarily to solve the power flow (PF) problem for cases that do not converge [45, 46, 47, 48, 49].

While convergence to a global minimum with probability one is guaranteed for a convex optimization problem [43], this is generally not true for nonconvex problems. In order to understand when homotopy can be effective in finding a global solution for nonconvex optimization, we explore a minimization problem of the form: $\min_x f(x)$ where $f : \mathbb{R}^n \to \mathbb{R}$ is a nonconvex function of $x \in \mathbb{R}^n$. This problem is named (P^o). Note that the function $f(\cdot)$ can incorporate exact/inexact penalty functions to enforce constraints on x, implying that this formulation is general for both unconstrained and constrained optimization [50]. We refer to (P^o) as the "base-case" problem. A deformed version of the base-case, which is also a nonconvex minimization problem, is denoted by (P^f) and defined as $\min_x \tilde{f}(x)$. For our application, (P^o) corresponds to the base-OPF problem and (P^f) corresponds to the contingency-OPF problem (the definition of these two problems are provided in the next section). We consider two possible methods for solving the deformed problem that are based on local search algorithms:

a) *One-shot method:* Use the solution of P^o as the initial point for any descent numerical algorithm to solve P^f.

b) *Homotopy method:* Generate a (discretized) homotopy map from P^o to P^f. Use the solution of P^o as the initial point, but update it at each step of the homotopy by solving an intermediate problem using local search that is initialized at the solution of the previous step. A linear (non-discretized) homotopy map can be defined as: $P(\lambda) = \min_x \left\{ \lambda \tilde{f}(x) + (1-\lambda) f(x) \right\}$, $0 \le \lambda \le 1$, with the property that $P(0) = P^o$ and $P(1) = P^f$.

Depending on $f(x)$ and $\tilde{f}(x)$, homotopy may or may not lead to better results than solving the deformed problem in one shot. In Figure 1, we see an example where homotopy is effective in finding the global minimum of a deformed problem and another example where it leads to a non-global local minimum. Knowing when homotopy will be effective is highly dependent on
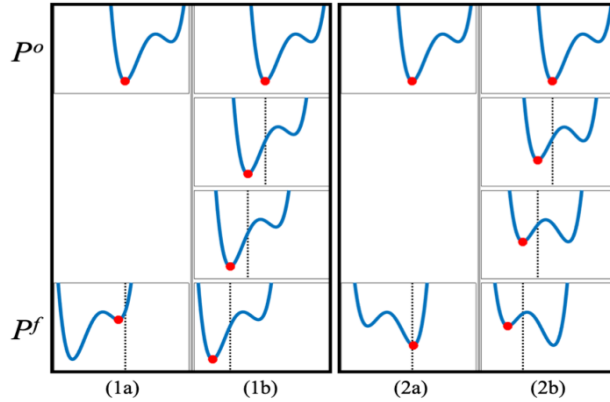
Figure 1 Evaluating the performance of homotopy on one-dimensional unconstrained minimization problems. The figure compares two different samples (1) and (2), with two different methods (a) and (b). The dotted lines show how the solution from the previous iteration is used in local search algorithms to solve the next problem. The red dots show the solution at each iteration using the position of the dotted lines as the initial point. For the one-shot method (a), the solution of P^o is used as the initial point for P^f. For the homotopy method (b), the base problem P^o is gradually transformed to P^f over three iterations, updating the initial point as the solution to the previous problem.

understanding how the shape of the function changes from the base-case to the deformed problem. In the current literature, there is a lack of theoretical results to characterize the performance of homotopy in finding a global optimum. While [43] presents algorithms that make use of homotopy to solve nonconvex, unconstrained minimization problems, these algorithms are similar to other stochastic search methods in that they do not guarantee convergence to the global minimum.

3. Formulation of Two-stage Security-constrained Optimal Power Flow

In this section, we present the mathematical formulation of the two-stage security-constrained OPF which is decomposed into the base-OPF and the contingency-OPF. The base-OPF resembles the conventional SCOPF that finds a base-case operational point which is robust against potential contingencies. The contingency-OPF focuses on a single contingency and attempts to find an adjusted operating point that minimizes constraint violations.

3.1. Base-case Optimal Power Flow

Recall that the *classic* optimal power flow problem (without security considerations) minimizes operating costs subject to technical limits, such as the power flow equations and explicit bounds on variables. The decision variables $x = (|v|, \theta, p^g, q^g) \in \mathbb{R}^{4|\mathcal{V}|}$ represent the vector of voltage magnitudes, voltage phase angles, real power generations and reactive power generations, corresponding to the pre-contingency base-case configuration of the network.

Now, suppose that there is a set of possible contingencies, namely $\mathcal{K}$, where each contingency corresponds to a line or generator outage. Each contingency $k \in \mathcal{K}$ introduces a new set of variables x^k, and therefore, for a network with $|\mathcal{V}|$ buses and $|\mathcal{K}|$ contingencies, the SCOPF problem will involve optimizing over $4|\mathcal{V}|(|\mathcal{K}|+1)$ scalar variables. The contingencies also add operational constraints of their own. In addition, there are physical limitations on how the post-contingency network can adapt from the base-case, and these limits are added as constraints that are functions of the base-case variables.

Since this extremely high-dimensional problem is cumbersome to solve, in practice the contingency constraints are approximated via methods such as LODF and PTDF [51]. In essence, this approximates the contingency variable x^k as a function of the base-case variable x. Therefore, post-contingency equality constraints for contingency k are approximated by a composite function of the form $h_k(x) \triangleq t_k(a_k(x))$, where $a_k(x)$ represents the control actions that are taken in the event of a contingency. The same goes for post-contingency inequality constraints, represented by $g_k(x)$.

Finally, another important consideration is how SCOPF performs when the problem is infeasible. Therefore, we model some operational limits using soft constraints with extra variables that capture the amount of violation. The objective function that is minimized is the sum of real power generation costs in the base-case as well as a weighted sum of equality constraint violation penalties in the contingencies. The standard optimization form is presented below:

$$
[\text{ base-OPF }] \quad \min_{x, \{\sigma_k\}} \quad f(x) + \sum_{k=1}^{|\mathcal{K}|} \phi_k(\sigma_k)
$$
$$
\text{s.t.} \quad h(x) = 0, \quad g(x) \leq 0
$$
$$
h_k(x) = \sigma_k, \ g_k(x) \leq 0, \quad \forall k \in \{1, \ldots, |\mathcal{K}|\} \tag{2}
$$

where $\phi_k(\cdot)$ represents the penalty functions for the violations. We denote this problem as the base-OPF.

3.2. Post-contingency Optimal Power Flow

The base-OPF solves for the base-case operating point by taking into account the possible failures in the network. In the process, it approximates the relationship between the contingency operation point x^k and the base-case operating point x. However, it does not actually solve for the optimal x^k's. Therefore, for each contingency we propose to solve a contingency-OPF problem to find the best operating point for the specific contingency scenario, given the base solution.

We model a contingency, such as a line or generator outage, by changing the system parameters from their base values. For example, a line outage physically means that power cannot flow over that connection, which can be modeled by setting the resistance of the line to infinity or its conductance

to zero. In the event of a line outage, the power is re-routed through other paths and therefore the amount of loss in the system changes. However, the difference in loss is small enough such that there is often no need for additional participation from other generators, unlike in the scenario of a generator outage. Therefore, we fix the real power generation to be equal to the base-case values and solve for the remaining variables such that the violations for the bus balance equations are small and spread out as much as possible (note that the proposed method can handle generator participation, if needed). This is because a large concentrated violation in a few buses can result in serious issues for the power network, whereas small power mismatches can be taken care of by real-time feedback controllers. Taking these into consideration, each contingency-OPF under study is given as

$$
\min_{|v|,\theta,q^g,\sigma^p,\sigma^q} \quad \phi(\sigma^p,\sigma^q)
$$

$$
\text{s.t.} \quad P_i^g - \sum_{j=1}^{|\mathcal{V}|} |v_i||v_j|\big(\widetilde{G}_{ij}\cos\theta_{ij} + \widetilde{B}_{ij}\sin\theta_{ij}\big) = P_i^d + \sigma_i^p \quad \forall i \in \mathcal{V}
$$

$$
q_i^g - \sum_{j=1}^{|\mathcal{V}|} |v_i||v_j|\big(\widetilde{G}_{ij}\sin\theta_{ij} - \widetilde{B}_{ij}\cos\theta_{ij}\big) = Q_i^d + \sigma_i^q \quad \forall i \in \mathcal{V}
$$

$$
|v_i| = |v_i|^{base} \qquad\qquad\qquad \forall i \in \mathcal{V}\setminus\mathcal{V}^q
$$

$$
Q_i^{min} \le q_i^g \le Q_i^{max} \qquad\qquad\qquad \forall i \in \mathcal{V}
$$

$$
V_i^{min} \le |v_i| \le V_i^{max} \qquad\qquad\qquad \forall i \in \mathcal{V}^q
$$

$$
|\theta_i - \theta_j| \le \Theta_{ij}^{max} \qquad\qquad\qquad \forall (i,j) \in \mathcal{E}
$$

(3)

Here, $\mathcal{V}^q$ is the set of buses that hit their upper or lower reactive power generation bounds in the base-case, and $|v_i|^{base}$ is the voltage magnitude of bus i in the base-case. The notations $\widetilde{G}_{ij}$ and $\widetilde{B}_{ij}$ reflect the potential change in the admittance matrix from the base-case values $Y_{ij} = G_{ij} + \mathbf{j}B_{ij}$. Note that real power generation is now a fixed parameter obtained from a solution of the base-OPF and therefore has been denoted by capital P^g. In the above formulation, constraints on the power flow over transmission lines are modeled as constraints on the angle differences between buses, which is a common practice [12]. However, the proposed method is general and can accommodate other types of line flow constraints.

For generator outage contingencies, there is an additional aspect to consider. A generator outage corresponds to setting the real power generation at that generator to zero. However, in order to compensate for the lost generation, the system operator needs to increase the power generation at other generators that participate in the outage response. The above framework is general enough to incorporate this difference: simply set $P^g = P^{g,f}$ and $\widetilde{G}_{ij} = G_{ij}, \widetilde{B}_{ij} = B_{ij}$ for all $(i,j) \in \mathcal{E}$, where $P^{g,f}$

is the new setpoint for the real power generation. Denoting $x = [|v|, \theta, q^g, \sigma^p, \sigma^q]$ as the combined variable, contingency-OPF in a standard optimization form would be:

$$[\text{ contingency-OPF }] \quad \min_x \quad f(x)$$
$$\text{s.t.} \quad h(x) = 0, \ g(x) \leq 0 \tag{4}$$

Note that $f(\cdot)$ is not the same objective function used for the base-OPF but merely a simplified notation for $\phi(\sigma^p, \sigma^q)$. With no loss of generality, we focus on the case when $\phi(\sigma^p, \sigma^q) = \sum_i \{c_i^p (\sigma_i^p)^2 + c_i^q (\sigma_i^q)^2\}$, where c_i^p and c_i^p are cost coefficients. Similarly, $h(\cdot)$ is the not the same as the constraint functions used for the base-OPF.

If the optimal objective value of the contingency-OPF is zero, it means that the solution of the base-case could be modified to stay feasible in case of the contingency. However, the primary focus of this paper is on hard instances with a nonzero optimal cost, meaning that some of the constraints must be violated to accommodate the outage. In these cases, since taking corrective actions to deal with nodal power violations is expensive, it is essential to find a global solution.

4. Methods

In the following subsections, we present a homotopy method that parametrizes the contingency-OPF to model a gradual line or a generator outage.

4.1. Homotopy Method for a Line Outage

In order to solve the contingency-OPF problem, we propose a homotopy method that gradually changes certain parameters of the problem from the base-OPF, rather than abruptly changing the structure of the network. For a line outage contingency, we introduce an aggregate homotopy parameter $\lambda = [\gamma, \beta, \gamma^{\text{sh}}, \beta^{\text{sh}}]$ corresponding to the series admittance and the shunt admittance, where $\gamma, \beta, \gamma^{\text{sh}}, \beta^{\text{sh}} \in \mathbb{R}^{|\mathcal{E}|}$. To be more precise, we parametrize the admittance in the contingency-OPF as follows:

$$y_{ij}(\lambda) = g_{ij}\gamma_{ij} + \mathbf{j}b_{ij}\beta_{ij} \qquad \forall (i,j) \in \mathcal{E} \tag{5a}$$

$$y_{ij}^{\text{sh}}(\lambda) = g_{ij}^{\text{sh}}\gamma_{ij}^{\text{sh}} + \mathbf{j}b_{ij}^{\text{sh}}\beta_{ij}^{\text{sh}} \quad \forall (i,j) \in \mathcal{E} \tag{5b}$$

which creates a family of OPF problems, named H_λ, written in the standard form of:

$$\begin{bmatrix} \text{homotopy-OPF} \\ H_\lambda \end{bmatrix} \quad \begin{aligned} \min_x \quad & f(x, \lambda) \\ \text{s.t.} \quad & h(x, \lambda) = 0, \ g(x, \lambda) \leq 0 \end{aligned} \tag{6}$$

Now, let $\ell \in \mathcal{E}$ be a line that connects buses i and j, and consider a contingency scenario in which the line ℓ is out. Notice that $\lambda^o = [\mathbf{1}_{|\mathcal{E}|}, \mathbf{1}_{|\mathcal{E}|}, \mathbf{1}_{|\mathcal{E}|}, \mathbf{1}_{|\mathcal{E}|}]$ corresponds to the original network before the line outage, and $\lambda^f = [\mathbf{1}_{|\mathcal{E}|}^\ell, \mathbf{1}_{|\mathcal{E}|}^\ell, \mathbf{1}_{|\mathcal{E}|}^\ell, \mathbf{1}_{|\mathcal{E}|}^\ell]$ corresponds to the post-contingency network after the line outage. By varying λ from λ^o to λ^f, the homotopy map allows us to create fictitious power networks that constitute a series of intermediate OPF problems.

4.2. Homotopy Method for a Generator Outage

For a generator outage, our proposed homotopy map gradually decreases the real power generation at the generators that are out and gradually increases the real power generation at the generators participating in the contingency response. For the simplicity of presentation, consider contingencies associated with a single generator (generator k) outage. This is common practice in power systems and is referred to as the $N-1$ criterion. Yet, note that the proposed method can easily be extended to multiple generator outages and is incorporated in Algorithm 2.

Let $P^{g,o} \in \mathbb{R}^{|\mathcal{V}|}$ be the real power generated at all generators in the base-case. Using the participation factors of generators that are still active in the contingency, we can compute $P^{g,f} \in \mathbb{R}^{|\mathcal{V}|}$, the real power generated at all generators after the contingency. Since generator k is down in this contingency scenario, $P_k^{g,f} = 0$. One possible method to choose the participation factors that determine $P^{g,f}$ is provided in the Appendix. Similar to what we did for line outage contingencies, we introduce an aggregate homotopy parameter $\lambda = [\gamma, \beta]$ with $\gamma, \beta \in \mathbb{R}^{|\mathcal{V}|}$ to create the following homotopy map:

$$P^g(\gamma) = P^{g,o} \odot \gamma + P^{g,f} \odot (\mathbf{1}_{|\mathcal{V}|} - \gamma) \tag{7a}$$

$$Q^d(\beta) = Q^{d,o} \odot \beta + Q^{d,f} \odot (\mathbf{1}_{|\mathcal{V}|} - \beta) \tag{7b}$$

Focusing on the first equation where we parametrize the real power generation, notice that $\lambda^o = [\mathbf{1}_{|\mathcal{V}|}, \mathbf{1}_{|\mathcal{V}|}]$ corresponds to the original network before the generator outage, and $\lambda^f = [\mathbf{0}_{|\mathcal{V}|}, \mathbf{0}_{|\mathcal{V}|}]$ corresponds to the post-contingency network after the generator outage. By varying λ from λ^o to λ^f, the homotopy map allows us to trace a gradual generator outage. Equation (7b) parametrizes the reactive power demand, and we will set the value $Q^{d,f} \simeq Q^{d,o}$. Although the justification for this extra parametrization is not clear for the moment, we will explain later that the parametrization needs to be of high enough dimension in order for the homotopy method to be effective. The series of homotopy problems have the same form as those for the line outage, given by Equation (6).

4.3. Implementation of Homotopy-OPF

The global minimum of the base-OPF is also a global minimum of H_{λ^o} because at $\lambda = \lambda^o$, the parameters of the homotopy-OPF corresponds to the pre-contingency network, for which the violations are zero. Starting with a solution to the base-OPF, we aim to iteratively solve a series of homotopy-OPF problems along a path of λ to eventually arrive at the contingency-OPF. Our implementation of solving a series of homotopy-OPF, as presented in the previous section, can be viewed as a one-parametric optimization problem by defining $\widetilde{f}(x,t) = f(x, \lambda(t))$, $\widetilde{h}(x,t) = h(x, \lambda(t))$ and $\widetilde{g}(x,t) = g(x, \lambda(t))$, where $\lambda(t)$ is a continuous function in t such that $\lambda(0) = \lambda^o$ and $\lambda(1) = \lambda^f$. The trajectory of λ's tracing from $\lambda(0)$ to $\lambda(1)$ is called the homotopy path. Then, the problem reduces

to solving the following problem for a suitable discretized partition of t in the range $[0, 1]$, namely $0 = t^1 \leq t^2 \leq \cdots \leq t^T = 1$:

$$\begin{bmatrix} \text{homotopy-OPF} \\ H_t \end{bmatrix} \qquad \begin{array}{ll} \min\limits_{x} & \widetilde{f}(x, t) \\ \text{s.t.} & \widetilde{h}(x, t) = 0, \ \widetilde{g}(x, t) \leq 0 \end{array} \qquad (8)$$

We make the following assumptions for the development of the results of this section:

(A_1) There exists a continuous function $x^*(t) : [0, 1] \to \mathbb{R}^{5|\mathcal{V}|}$ such that $x^*(t)$ is a global minimizer for H_t. Moreover, $x^*(0)$ is unique and known.

(A_2) There exists a neighborhood U of $\{(x^*(t), t)\} \subset \mathbb{R}^{5|\mathcal{V}|} \times [0, 1]$ such that for all $(x, t) \in U$, the functions $\widetilde{f}$ and $\widetilde{h}$ are twice continuously differentiable with respect to x.

(A_3) Linear independence constraint qualification (LICQ) and strong second-order sufficient conditions (SSOC) are satisfied at $x^*(t)$ for every $t \in [0, 1]$.

Note that the discretization of homotopy path can also be represented by the set $\Lambda := \{\Lambda^1, \ldots, \Lambda^T\}$, where $\Lambda^i = \lambda(t^i)$ for $i = 1, \ldots, T$, $\Lambda^1 = \lambda(t^1) = \lambda^o$ and $\Lambda^T = \lambda(t^T) = \lambda^f$. In other words, $H_{t^i} = H_{\Lambda^i}$. The SSOC is similar to the second-order sufficient conditions for local optimality but with the addition of the strict complementary slackness condition and the linear independence of the active constraints [52]. Furthermore, Assumptions $(A2)$ and $(A3)$ together imply that the Lagrange multipliers associated with $x^*(t)$ are uniquely determined for every $t \in [0, 1]$. We will later discuss that these assumptions are mild.

To begin, the first homotopy-OPF problem H_{t^1} is initialized as the solution to the base-OPF problem. The series of homotopy-OPF problems are then solved sequentially, where the solution to the previous homotopy-OPF problem H_{t^i} is utilized as the initial point for a local search algorithm solving $H_{t^{i+1}}$. Please refer to Algorithms 1 and 2 for complete details of the method.

In this paper, we assume that the base-OPF has a unique global minimum that is available (known). The availability of a global minimum is a reasonable assumption because a good initial point is usually provided for the base-OPF, and also because more time is allocated to solving it compared to a large number of contingency-OPF problems for different outages, allowing the use of various convex relaxation techniques for the base-OPF. If the optimal violation cost for H_{λ^o} is nonzero, the global minimum will be unique with overwhelming probability. Furthermore, even if the violation cost is zero, it will immediately become nonzero during the next homotopy iteration if removing a line or generator introduces inflexibilities that the network cannot accommodate. In fact, these near-infeasible problems where a contingency will make the system "stressed" are the cases where homotopy can be useful and are the focus of this paper. Later in the paper, we will present a rigorous result showing that the uniqueness of the global minimum is a generic property for H_λ.

Algorithm 1 Homotopy-OPF for Line Outages

   Given: Contingency set $\mathcal{K}$ with line outages $L_k \subset \mathcal{E}$ for each $k \in \mathcal{K}$

   Initialize: Solve base-OPF problem to find a globally optimal solution $(|v|_*, \theta_*, p_*^g, q_*^g, \{\sigma_{k*}\})$.

   Formulate the contingency-OPF problem:

      1. Fix real power generation to base-case solution: $P^g := p_*^g$

      2. Find $\mathcal{V}^q$ based on q_*^g.

   for $k \in \mathcal{K}$ **do**

      Set up homotopy-OPF family H_Λ for given line outages L_k.

      Initialize $(|\tilde{v}|, \tilde{\theta}, \tilde{q}^g, \tilde{\sigma}^p, \tilde{\sigma}^q)$ as the solution of base-OPF.

      for $i \in \{1, ..., T\}$ **do**

         Solve H_{Λ^i} using initial point $(|\tilde{v}|, \tilde{\theta}, \tilde{q}^g, \tilde{\sigma}^p, \tilde{\sigma}^q)$, and obtain new solution $(|v|, \theta, q^g, \sigma^p, \sigma^q)$.

         Update $(|\tilde{v}|, \tilde{\theta}, \tilde{q}^g, \tilde{\sigma}^p, \tilde{\sigma}^q) \leftarrow (|v|, \theta, q^g, \sigma^p, \sigma^q)$

      end for

      Return $(|v|, \theta, q^g, \sigma^p, \sigma^q)$ and violation cost $\phi(\sigma^p, \sigma^q)$.

   end for

---

5. Analysis of Homotopy Paths

In Section 2, we offered two examples of nonconvex optimization: one in which the homotopy method resulted in the global minimum and another in which the homotopy method resulted in a non-global local minimum (see Figure 1). In this section, we describe a theoretical framework that describes when homotopy can be used to obtain a global minimum. We apply this framework to analyze the performance of homotopy-OPF in finding the global solution of the contingency-OPF. The results developed in this section have implications for homotopy methods in a broad range of optimization problems.

THEOREM 1. *Let $\bar{x}(t^i, z)$ denote the stationary point of H_{t^i} that a local search algorithm converges to when initialized at point z. Set $z^1 = x^*(t^1) := x^*(0)$ and consider the sequence of points $\{x(t^i)\}_{i=1}^T$ generated by the following update rule:*

$$x(t^i) = \bar{x}(t^i, z^i) \tag{9}$$

$$z^{i+1} = x(t^i) \tag{10}$$

Moreover, define $\Delta t := \sup_{i=1,\ldots,T-1}(t^{i+1} - t^i)$. Under Assumptions (A1), (A2) and (A3), a sufficiently small Δt will ensure that $x(t^i)$ is a global minimizer of H_{t^i} for $i = 1, \ldots, T$.

Theorem 1 states that if we can solve each H_t exactly, then a sufficiently small stepsize in the parameter t (or equivalently λ) can track the global minimizer from the base-OPF all the way to the contingency-OPF. However, an exact solution to each H_t (or equivalently H_λ) is generally

---

Algorithm 2 Homotopy-OPF for Generator Outages

   Given: Contingency set $\mathcal{K}$ with generator outages $R_k \subset \mathcal{V}$ for each $k \in \mathcal{K}$

   Initialize: Solve base-OPF problem to find a globally optimal solution $(|v|_*, \theta_*, p_*^g, q_*^g, \{\sigma_{k*}\})$.

   for $k \in \mathcal{K}$ **do**

       Formulate the contingency-OPF problem:

       Define P_r^g as the fixed real power generation at $r \in \mathcal{V}$

       Define ΔP_k^g as the total lost real power generation at k: $\Delta P_k^g := \sum_{r \in R_k} p_{*,r}^g$

       1. Find $\mathcal{V}^q$.

       2. Remove real power generation for generators in R_k: $P_r^g \leftarrow 0 \quad \forall r \in R_k$

       3. Compute participation factors α_r^g for $r \in \mathcal{V} \setminus R_k$ (see Algorithm 3 in the Appendix)

       4. Add real power generation for participating generators:

       for $r \in \mathcal{V} \setminus R_k$ **do**

           if $\alpha_r^g > 0$ **then**

               $P_r^g \leftarrow \max\{\alpha_r^g \Delta P_k^g, P_r^{max} - p_{*,r}^g\}$

           end if

       end for

       Set up homotopy-OPF family H_Λ for given generator outages R_k.

       Let $P^{g,o} := p_*^g$ and $P^{g,f} := P^g$

       Initialize $(|\tilde{v}|, \tilde{\theta}, \tilde{q}^g, \tilde{\sigma}^p, \tilde{\sigma}^q)$ as the solution of base-OPF.

       for $i \in \{1, ..., T\}$ **do**

           Solve H_{Λ^i} using initial point $(|\tilde{v}|, \tilde{\theta}, \tilde{q}^g, \tilde{\sigma}^p, \tilde{\sigma}^q)$ and obtain new solution $(|v|, \theta, q^g, \sigma^p, \sigma^q)$

           Update $(|\tilde{v}|, \tilde{\theta}, \tilde{q}^g, \tilde{\sigma}^p, \tilde{\sigma}^q) \leftarrow (|v|, \theta, q^g, \sigma^p, \sigma^q)$

       end for

       Return $(|v|, \theta, q^g, \sigma^p, \sigma^q)$ and violation cost $\phi(\sigma^p, \sigma^q)$

   end for

---

unattainable in practice. Furthermore, the interplay between the accuracy of solving each H_t and the number of discretization contribute to the overall complexity of solving homotopy-OPF. We will show that it suffices to find an approximate solution with not a necessarily high accuracy. This will significantly reduce the complexity of solving the parametric homotopy-OPF.

5.1. Convergence and Complexity of Homotopy-OPF

In this subsection, we analyze the complexity of solving the contingency-OPF using the proposed homotopy method. The results here are based on a specific local search algorithm called Wilson's method. However, there are many other methods, such as Robinson's method, that can achieve the same results [53]. Let μ and ζ denote the Lagrange multipliers for the constraints $\widetilde{h}(x, t) = 0$ and

$\widetilde{g}(x,t) \leq 0$, respectively. For every instance of H_t, we determine a local minimizer and its Lagrange multipliers, $w(t) = (x(t), \mu(t), \zeta(t))$ by using the following Wilson's method: Start with an initial point w^0, and solve the optimization problem $W(w^k, t)$ in order to find the next iterate w^{k+1} for $k \in \{0, 1, 2, \ldots\}$, where the problem $W(w^k, t)$ is defined below.

$$W(w^k, t): \quad \min_x \quad \nabla_x \widetilde{f}(x^k, t)^T (x - x^k) + \frac{1}{2}(x - x^k)^T \nabla_x^2 \widetilde{L}(w^k, t)(x - x^k) \tag{11a}$$

$$\text{s.t.} \quad \widetilde{h}_i(x^k, t) + \nabla_x \widetilde{h}_i(x^k, t)^T (x - x^k) = 0, \ \forall i \in \mathcal{I} \tag{11b}$$

$$\widetilde{g}_j(x^k, t) + \nabla_x \widetilde{g}_j(x^k, t)^T (x - x^k) \leq 0, \ \forall j \in \mathcal{J} \tag{11c}$$

where $\mathcal{I}$ and $\mathcal{J}$ denote the set of indices for the equality constraints and inequality constraints, respectively, and $\widetilde{L}(w^k, t) = \widetilde{f}(x^k, t) + \sum_i \mu_i^k \widetilde{h}_i(x^k, t) + \sum_i \zeta_i^k \widetilde{g}_i(x^k, t)$. Furthermore, let a global minimizer of H_t and its corresponding Lagrange multipliers be denoted by $w^*(t) = (x^*(t), \mu^*(t), \zeta^*(t))$. In this problem, we solve for the optimization variable x and the Lagrange multipliers associated with (11b) and (11c) to be able to find a primal-dual solution. Let us define the function $\hat{w}(w^k, t)$ as the exact solution to $W(w^k, t)$. Then, w^{k+1} numerically approximates $\hat{w}(w^k, t)$. The process is repeated for increasing values of k until a predefined criteria is met, and the final iterate of $\{w^k\}$ is returned as an approximate solution to $w(t)$.

THEOREM 2. *Suppose that Assumptions* $(A1), (A2)$ *and* $(A3)$ *hold. Consider the following algorithm for a constant number M: Given $w_0 = w^*(t^1) := (x^*(t^1), \mu^*(t^1), \zeta^*(t^1))$, compute w_i as the solution to H_{t^i} using M Wilson's iterations starting at w_{i-1} for $i = 1, \ldots, T$. There exist positive constants $\hat{r}$ and Δt such that for every sufficiently small $\epsilon > 0$, the algorithm generates points $\{w_i'\}_{i=1}^T$ with $\|w_i' - w^*(t^i)\| < \epsilon$ whenever $t^{i+1} - t^i \leq \Delta t$ for $i = 1, 2, \ldots, T$, provided that M is chosen to be larger than $\log(\hat{r}/\epsilon)$. In particular, the Wilson complexity (total number of Wilson steps) of finding an almost globally optimal solution with ϵ error for H_{t^T} is $O(\log(1/\epsilon))$.*

The above theorem implies that given a global minimizer for the initial problem H_{t^1}, we can simply solve a small number of convex quadratic programs for each H_{t^i} and keep track of its global minimizers. In particular, the quadratic program (11) is convex because the SSOC holds at the global minimizers. Furthermore, the number of parameter discretizations needed is upper bounded by a constant for small values of ϵ. This result is aligned with the complexity analysis of interior-point methods [54]. More insight is provided in the proof.

REMARK 1. *Our assumptions imply that H_t along $\lambda(t)$ has a unique global solution satisfying SSOC. In the next subsection, we argue that this is a reasonable assumption to make. In addition, this assumption on the global solution can be replaced by the "connectivity" of the set of all global solutions (this allows having infinitely many possible solutions for post-contingency OPF with zero violation cost). In what follows, we show that the uniqueness of the global minimum is a generic property for H_t.*

5.2. Genericity of Unique Global Minimizer with SSOC

Recall that a set $\mathbb{S} \subset \mathbb{R}^n$ has (Lebesgue) measure zero if for every $\epsilon > 0$, $\mathbb{S}$ can be covered by a countable union of n-cubes, the sum of whose measures is less than ϵ. A property that holds except on a subset whose Lebesgue measure is zero is said to be satisfied *generically* or hold for *almost all*. In this subsection, we will show that the homotopy-OPF generically has a unique global minimizer that satisfies SSOC .

Consider the following family of problems, which adds a linear perturbation to the objective of the homotopy-OPF:

$$\left[H_{\lambda,\omega}\right] \qquad \begin{array}{ll} \min\limits_{x \in \Psi} & f(x,\lambda) + \omega^T x \\ \text{s.t.} & h(x,\lambda) = 0 \end{array} \tag{12}$$

where $f : \mathbb{R}^{5|\mathcal{V}|} \times \mathbb{R}^\ell \to \mathbb{R}$, $h : \mathbb{R}^{5|\mathcal{V}|} \times \mathbb{R}^\ell \to \mathbb{R}^{2|\mathcal{V}|}$ are smooth functions and the parameters (λ, ω) belong to an open set $\mathbb{U} \subset \mathbb{R}^\ell \times \mathbb{R}^{5|\mathcal{V}|}$. The set $\Psi \subset \mathbb{R}^{5|\mathcal{V}|}$ is defined as below:

$$\Psi = \left\{ (|v|, \theta, q^g, \sigma^p, \sigma^q) \,\middle|\, \begin{array}{ll} Q_i^{min} \leq q_i^g \leq Q_i^{max} & \forall i \in \mathcal{V} \\ V_i^{min} \leq |v_i| \leq V_i^{max} & \forall i \in \mathcal{V}^q \\ |\theta_i - \theta_j| \leq \Theta_{ij}^{max} & \forall (i,j) \in \mathcal{E} \\ |v_i| = |v_i|^{base} & \forall i \in \mathcal{V} \backslash \mathcal{V}^q \end{array} \right\} \tag{13}$$

This formulation is possible by noticing that the inequality constraints of homotopy-OPF are independent of the parameter λ. We call this problem the extended homotopy-OPF. Here, ℓ represents the dimension of the parameter λ, which can be equal to either $4|\mathcal{E}|$ (for line contingencies) or $2|\mathcal{V}|$ (for generator contingencies). Then, using the results from [52], we can easily derive the following lemma:

LEMMA 1. *Suppose that the following two conditions are satisfied:*

1. *The function $\lambda \to h(x,\lambda)$ is of full rank $2|\mathcal{V}|$ for all $x \in \Psi$ at every λ [1].*
2. *The set Ψ is a cyrtohedron and the set $\mathbb{U}$ is an open set.*

Then, for almost all (λ, ω) except those in a set $\mathbb{U}' \subset \mathbb{U}$ of measure zero, $H_{\lambda,\omega}$ has a unique global minimizer satisfying SSOC. In fact, for every $(\lambda, \omega) \in \mathbb{U} \backslash \mathbb{U}'$, $H_{\lambda,\omega}$ cannot achieve the same objective value at any two distinct critical points.

The concept of a cyrtohedra was first introduced in [55] and it captures a class of sets whose boundaries are a union of countably many smooth manifolds pieced together. A few main examples of cyrtohedra include polyhedral convex sets, submanifolds, submanifolds with boundaries, and manifolds with corners. In our case, the set Ψ is naturally a cyrtohedra and therefore we only have to verify the first condition. The next lemma proves that the condition can be easily verified for the line outage contingency.

---

[1] The rank of a differentiable mapping is the rank of its Jacobian.

LEMMA 2. *Define the matrix* $J = \left[\begin{array}{c|c} J^1 & 0 \\ \hline 0 & J^2 \end{array}\right] \in \mathbb{R}^{2|\mathcal{E}| \times 2|\mathcal{V}|}$ *as*

$$J^1_{(i,j),k} = \begin{cases} -\frac{1}{2} g^{sh}_{ij} |v_k|^2 & \text{for } k = i \text{ or } j, \ j \in \mathcal{N}(i) \\ 0 & \text{otherwise} \end{cases}$$

$$J^2_{(i,j),k} = \begin{cases} \frac{1}{2} b^{sh}_{ij} |v_k|^2 & \text{for } k = i \text{ or } j, \ j \in \mathcal{N}(i) \\ 0 & \text{otherwise} \end{cases}$$

where the column and row indices represent the lines and the nodes of the power system, respectively. If J has full column rank, then the function $\lambda \to h(x, \lambda)$ associated with the line outage homotopy method is of full rank $2|\mathcal{V}|$.

A similar result holds for generator outage contingencies, as shown below.

LEMMA 3. *Define the matrix* $M = \left[\begin{array}{c|c} M^1 & 0 \\ \hline 0 & M^2 \end{array}\right] \in \mathbb{R}^{2|\mathcal{V}| \times 2|\mathcal{V}|}$ *as*

$$M^1_{i,j} = \begin{cases} P^{g,o}_i - P^{g,f}_i & \text{for } j = i \\ 0 & \text{otherwise} \end{cases}$$

$$M^2_{i,j} = \begin{cases} Q^{d,o}_i - Q^{d,f}_i & \text{for } j = i \\ 0 & \text{otherwise} \end{cases}$$

where both the column and row indices represent the nodes of the power system network. If M has full rank, then the function $\lambda \to h(x, \lambda)$ associated with the generator outage homotopy method is of full rank $2|\mathcal{V}|$.

The result implies that the first condition of Lemma 1 is satisfied if: (i) the pre-contingency real power generations and the post-contingency real power generations are different and (ii) the pre-contingency reactive power demands and the post-contingency reactive power demands are different. Note that this does not necessarily hold true because some real power generations are supposed to be fixed even after the contingency (same for reactive power demand). However, we can address this issue by allowing $P^{g,f}_i$ ($Q^{d,f}_i$) to take on a value within a small interval around $P^{g,o}_i$ ($Q^{d,o}_i$) whenever we want the two values to be close to each other.

Note that the linear perturbation term in $H_{\lambda,\omega}$ is a mathematically necessary device that allows us to prove generic uniqueness of a family of nonlinear optimization problems. Ultimately, we will only consider very small perturbations so that $H_{\lambda,\omega}$ closely resembles H_λ. Using the lemmas above, we arrive at the following corollary:

COROLLARY 1. *Let $\mathbb{U}(\delta) = \{(\lambda, \omega) \mid \lambda \in \mathbb{S}, \ \omega \in \mathcal{B}(\delta)\}$, where $\mathbb{S}$ is an open set such that $[0,1]^m \subset \mathbb{S}$ and $\mathcal{B}(\delta)$ is an open n-dimensional ball around the origin with radius δ. Suppose that J and M have full column rank. Then, for every $\delta > 0$, $H_{\lambda,\omega}$ has a unique global minimizer satisfying SSOC for all $(\lambda, \omega) \in \mathbb{U}(\delta) \setminus \mathbb{U}'(\delta)$, where $\mathbb{U}'(\delta) \subset \mathbb{U}(\delta)$ is of measure zero.*

In other words, the uniqueness of a global minimizer satisfying SSOC is a generic property of H_λ, and thus supporting the assumptions made in this paper (specifically Assumptions ($A1$) and ($A3$)).
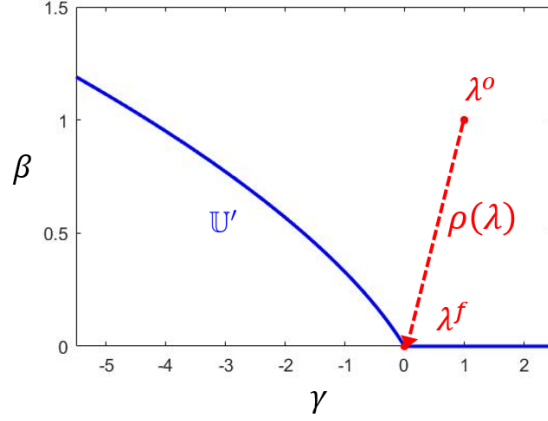
Figure 2   An example of the set $\mathbb{U}'$ (blue) and an effective homotopy path (red) that can reach the origin without passing through a point in $\mathbb{U}'$.

5.3. Geometry of the homotopy path: Two-bus example

In order to illustrate the previous ideas, we consider a simple homotopy-OPF example on a two-bus system. The line connecting the two buses has the admittance $y = G\gamma - \mathbf{j}B\beta$, and there is a lower bound Q^{min} on the reactive power injections at both buses. In this two-bus example, we consider the objective function $(\sigma_1^p)^2 + c(\sigma_2^p)^2$. Furthermore, assume that:

1. $|v_1| = |v_2| = 1$
2. $-\Delta' \leq \theta_1 - \theta_2 \leq \Delta'$
3. $0 < Q^{min} < q(\Delta')$

where $\Delta' = \tan^{-1}(B\beta/G\gamma)$ and $q(\cdot)$ denotes the reactive power injection as a function of solely the angle difference, which is due to the fact that voltage magnitudes are fixed. Note that the second constraint on the angle difference is reasonable for the secure operation of power systems and is also used in [11] in order to restrict the two-bus real power injection region to be the Pareto front of the original feasible region. Geometrically, the feasible set of the two-bus injection region is the Pareto front of an ellipse, which is partially removed due to the reactive power constraints (the details can be found in [11]). Let $P_i^{\mathrm{g,b}}$ denote the real power generation at bus i obtained from the base-OPF solution. The following lemma characterizes the set of homotopy parameters for which there are at least two global solutions.

LEMMA 4. *Denote* $\alpha = \cos^{-1}\left(\frac{-Q^{min} + B\beta}{|y|}\right)$, *and define two polynomial functions of* $\lambda = (\gamma, \beta)$ *as follows:*

$$\Omega_1(\gamma, \beta) = \frac{2B\beta}{|y|}\big(B\beta \cdot \sin\alpha + \alpha \cdot G\gamma\big) \tag{14}$$

$$\Omega_2(\gamma, \beta) = 2G\gamma - \frac{2G\gamma}{|y|}\big(-G\gamma \cdot \sin\alpha + \alpha \cdot B\beta\big) \tag{15}$$

Then, the set of parameters leading to multiple global minimizers, $\mathbb{U}'$, can be characterized as:

$$\mathbb{U}' = \{\lambda \in \mathbb{R}^2 \mid (1-c) \cdot \Omega_1(\gamma, \beta) \cdot \Omega_2(\gamma, \beta)$$
$$- 2(P_1^{g,b} - P_1^d) \cdot \Omega_1(\gamma, \beta) + 2c(P_2^{g,b} - P_2^d) \cdot \Omega_1(\gamma, \beta) = 0\} \tag{16}$$

The set $\mathbb{U}'$ in Lemma 4 for a particular instance of the example is depicted in Figure 2. As we can observe, $\mathbb{U}'$ is a measure zero set in the two-dimensional parameter space, and it is possible to design an effective homotopy path. Note that the linear perturbation term in $H_{\lambda, \omega}$ is a mathematical device used to prove generic uniqueness of the global minimizer for a family of problems. The characterization of $\mathbb{U}'$ in Lemma 4 did not require the linear perturbation. However, this means that particular instances of the example may not lead to the result that we desire. For instance, if $c = 1$ and $P_1^{g,b} - P_1^d = P_2^{g,b} - P_2^d$ in the above example, $\mathbb{U}'$ is no longer a measure-zero set.

6. Simulations

In this section, we numerically evaluate different homotopy paths and discretizations. We present simulations of different line and generator outage scenarios on various networks. The results from these simulations are consistent with the notion that the final violation cost is heavily dependent on the choice of the homotopy path.

In these simulations, we consider $N-1$ contingencies wherein there is one line or generator out as well as $N-2$ and $N-3$ contingencies wherein there are multiple outages. Although $N-1$ contingencies occur more frequently in practice, $N-2$ and $N-3$ contingencies are catastrophic events that are worth considering as they are harder to correct. Extreme weather events, attacks, or component aging could cause these $N-k$ (where $k \geq 2$) contingency scenarios to occur [56]. Adding uncertain renewable energy sources such as wind energy to power networks increases the probability of correlated faults and thus the possibility of $N-2$ and $N-3$ contingencies [57]. Additionally, these multi-contingency scenarios can capture cascading failures that occur in a short window where corrective action is not possible between contingencies [57].

In order to implement the contingency-OPF using the MATPOWER format [58], we introduce virtual generators that model the violations of real and reactive power balances at all nodes after an outage occurs. These violations are penalized in a modified objective function. The benefit of this formulation is that there always exists a feasible solution to contingency-OPF. By adding power generation flexibility with virtual generators, we aim to find a feasible point (equivalent to a zero objective value) or an infeasible point for the network but with the minimum violations (such solutions could yet be implemented via corrective actions taken by real-time feedback controllers). To solve each of the homotopy simulations, we use the MATPOWER Interior Point Solver (MIPS) [59].

For the line outages, we consider three different homotopy paths. If we take the line connecting buses i and j to be out, then the three homotopy paths are given by:
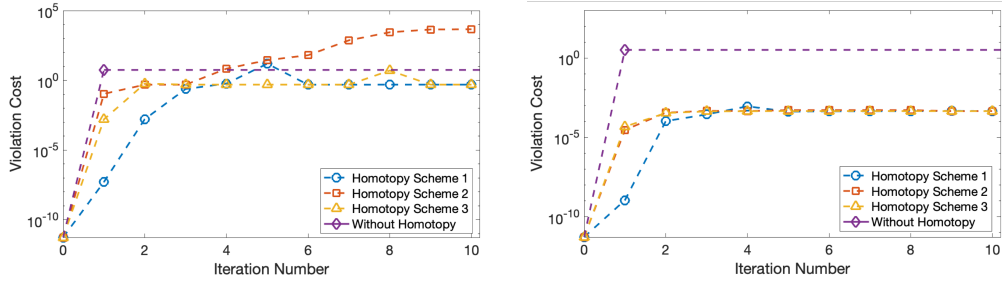
Figure 3   Performance of proposed homotopy method on the 3120-bus Polish network (`case3120sp` with real and reactive power demand scaled up by 10%) with a multiple line outages. Homotopy schemes 1 through 3 are tested with 10 iterations. By introducing multiple line outages, we make the contingency-OPF problem more difficult to solve, which makes it a good candidate for the proposed homotopy method. In the left figure, the IDs of the outed lines are 31 and 32, and in the right figure, the IDs of the outed lines are 438, 439, and 3150.
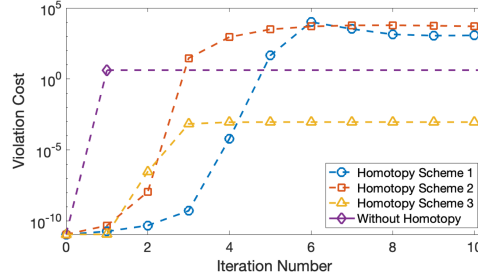

Figure 4   Performance of proposed homotopy method on the 3120-bus Polish network (`case3120sp` with original real and reactive power demand) with a single line outage (line out ID: 1602). Homotopy schemes 1 through 3 are tested with 10 iterations. In this example, homotopy schemes 1 and 2 result in an objective value higher than that obtained by the one-shot method, while the third homotopy scheme outperforms the one-shot method.

- Scheme 1: Uniformly decrease $(\gamma_{ij}, \beta_{ij})$ from $(1,1) \to (0,0)$
- Scheme 2: Decrease γ_{ij} from $1 \to 0$, then β_{ij} from $1 \to 0$
- Scheme 3: Decrease β_{ij} from $1 \to 0$, then γ_{ij} from $1 \to 0$

These schemes can be applied to multiple line outages by simultaneously modifying γ_{ij} and β_{ij} for each line $(i,j) \in \mathcal{E}$ that is out. For line outage scenarios on the 3120-bus Polish network, Figures 3 and 4 show the evolution of the violation cost over these homotopy schemes (with a 10-iteration discretization) compared to the violation cost of the one-shot method [58]. Next, we consider changing the discretization of homotopy scheme 1 in a line outage scenario. Figure 5 shows line outage scenarios on the 3012-bus Polish network using homotopy scheme 1 with a varying number of iterations [58].

For generator outages, we implement a homotopy path that decreases λ from $[\mathbf{1}_{|\mathcal{V}|}, \mathbf{1}_{|\mathcal{V}|}]$ to $[\mathbf{0}_{|\mathcal{V}|}, \mathbf{0}_{|\mathcal{V}|}]$ uniformly throughout the iterations. For this homotopy path, we also consider varying
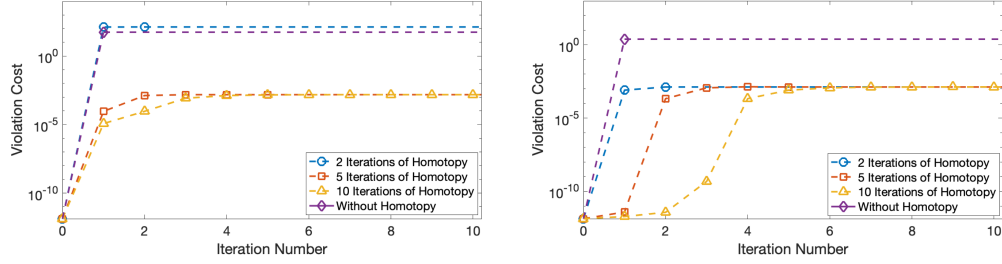
Figure 5 Performance of proposed homotopy method on the 3012-bus Polish network (`case3012wp` with real and reactive power demand scaled up by 8%) with single line outages. Homotopy scheme 1 is tested with a varying number of homotopy iterations. In the left figure (line out ID: 332), we see a case where the one-shot and 2-iteration homotopy methods result in much higher objective values than the 5 and 10-iteration homotopy methods. In the right figure (line out ID: 1604), we see a case where the 2, 5, and 10-iteration homotopy methods result in an objective value much lower than that obtained by the one-shot method. For this scenario, by introducing even a 2-iteration homotopy scheme we outperform the one-shot method.
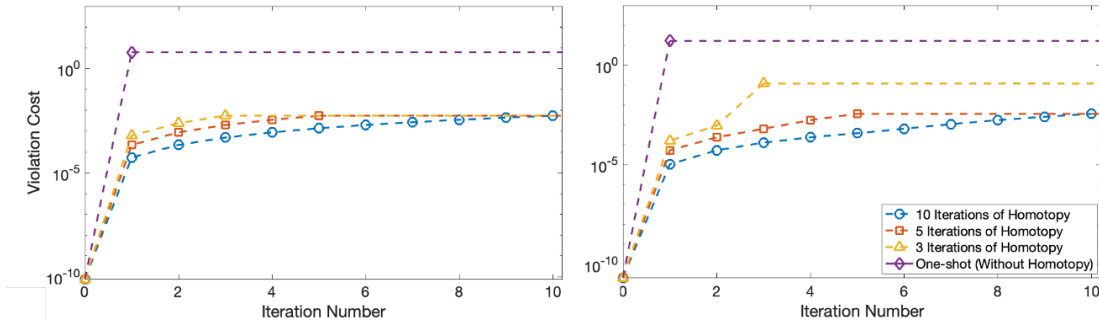

Figure 6 Performance of proposed homotopy method for generator outages. The left figure shows a 2 generator outage (generator out IDs: 4 and 7) in the 89-bus PEGASE network (`case89pegase`). The right figure shows a 1 generator outage (generator out ID: 30) in the 1354-bus PEGASE network (`case1354pegase`).

the discretization of the path. Figure 6 shows generator outage scenarios on the 89-bus and 1354-bus PEGASE networks [60, 61]. From these figures, we can see that the final violation cost obtained using the given homotopy paths can vary significantly depending on the number of iterations (i.e. $\Delta\lambda$) of homotopy-OPF.

In order to formally compare the performance of homotopy versus the one-shot method, we say that homotopy "outperforms" the one-shot method if either of the following are true:

1. If the homotopy scheme converges and the one-shot method does not converge.
2. If the homotopy scheme converges to a value that is better than that of the one-shot method by at least 0.01% of the optimal base-OPF cost.

For the 1354-bus PEGASE network, we tested 1, 2, and 3 line and generator outages, testing 100 simulations of each type of outage. The homotopy paths for these line and generator outages

Table 1   Percent of simulations where 5-iteration homotopy scheme outperformed one-shot method for 1354-bus PEGASE network

Type of contingency	Base-level power demand	10% greater power demand
1 line outage	10%	12%
2 line outage	7%	12%
3 line outage	12%	15%
1 generator outage	9%	7%
2 generator outage	10%	9%
3 generator outage	17%	12%

are the same as those described for the simulations in Figures 5 and 6. The percent of simulations where homotopy outperformed the one-shot method is given in Table 1 for the network with base-level demand and with demand scaled up by 10%. It can be observed that for the line outage contingencies, the homotopy methods appear to be more useful when the demand is higher. This is likely because the increased demand makes the problem harder, and thus homotopy is more useful. However, the inverse appears true for the generator outage scenarios, i.e. the homotopy methods appear to be more useful when demand is at the base-level. This could be because the removal of a generator could lead to many possibilities for operating the post-contingency network in a lower demand scenario, which may introduce bad local minima.

Although the percent of simulations where homotopy outperforms the one-shot method is less than 20% for the considered cases, it is important to note that in these cases the homotopy method can lead to a significant reduction in the violation cost during a contingency scenario. For the cases where the proposed homotopy method does not outperform the one-shot method, the homotopy method typically is at least as good as the one-shot method.

7. Conclusions

This paper studies the contingency-OPF problem, which is used to find an optimal operating point in the case of a line or generator outage. Unlike the base-OPF problem that is a single optimization problem, there are many contingency-OPF problems that should all be solved in a short period of time. Recognizing that the contingency-OPF problem is a challenging variant of the classical OPF problem, we introduce a new homotopy method to find the best solution of the contingency-OPF problem. This method involves solving a series of intermediate homotopy-OPF problems using simple local search methods, and we study conditions that guarantee convergence to a global solution of the contingency-OPF. We perform simulations on real-world networks and show that the proposed homotopy method can result in a lower value of the objective.

References

[1] S. Park, E. Glista, J. Lavaei, and S. Sojoudi, "Homotopy method for finding the global solution of post-contingency optimal power flow," *American Control Conference*, 2020.

[2] J. Carpentier, "Contribution to the economic dispatch problem," *Bulletin de la Societe Francoise des Electriciens*, vol. 3, no. 8, pp. 431–447, 1962.

[3] A. J. Wood, B. F. Wollenberg, and G. B. Sheblé, *Power generation, operation and control.* Wiley, 2014.

[4] A. Conejo and J. Aguado, "Multi-area coordinated decentralized DC optimal power flow," *IEEE Transactions on Power Systems*, vol. 13, no. 4, pp. 1272–1278, 1998.

[5] G. Torres and V. Quintana, "An interior-point method for nonlinear optimal power flow using voltage rectangular coordinates," *IEEE Transactions on Power Systems*, vol. 13, no. 4, pp. 1211–1218, 1998.

[6] R. A. Jabr, "A primal-dual interior-point method to solve the optimal power flow dispatching problem," *Optimization and Engineering*, vol. 4, pp. 309–336, 2003.

[7] E. J.Oliveira, L. W.Oliveira, J.L.R.Pereira, L. M.Honório, I. C. Junior, and A.L.M.Marcato, "An optimal power flow based on safety barrier interior point method," *International Journal of Electrical power & energy systems*, vol. 64, pp. 977–985, 2015.

[8] J. Lavaei and S. H. Low, "Zero duality gap in optimal power flow problem," *IEEE Transactions on Power Systems*, vol. 27, no. 1, pp. 92–107, 2012.

[9] S. Sojoudi and J. Lavaei, "Physics of power networks makes hard optimization problems easy to solve," in *Power and Energy Society General Meeting*, 2012, pp. 1–8.

[10] M. Farivar and S. H. Low, "Branch flow model: Relaxations and convexification—part I," *IEEE Transactions on Power Systems*, vol. 28, no. 3, pp. 2554–2564, 2013.

[11] J. Lavaei, D. Tse, and B. Zhang, "Geometry of power flows and optimization in distribution networks," *IEEE Transactions on Power Systems*, vol. 29, no. 2, pp. 572–583, 2014.

[12] R. Madani, S. Sojoudi, and J. Lavaei, "Convex relaxation for optimal power flow problem: Mesh networks," *IEEE Transactions on Power Systems*, vol. 30, no. 1, pp. 199–211, 2015.

[13] R. Madani, M. Ashraphijuo, and J. Lavaei, "Promises of conic relaxation for contingency-constrained optimal power flow problem," *IEEE Transactions on Power Systems*, vol. 31, no. 2, pp. 1297–1307, 2016.

[14] C. Chen, A. Atamtürk, and S. Oren, "A spatial branch-and-cut method for nonconvex QCQP with bounded complex variables," *Mathematical Programming*, 2016.

[15] C. Josz, J. Maeght, P. Panciatici, J. C. Gilbert, "Application of the moment-SOS approach to global optimization of the OPF problem," *IEEE Transactions on Power Systems*, vol. 30, no. 1, pp. 463–470, 2015.

[16] D. K. Molzahn and I. A. Hiskens, "Sparsity-exploiting moment-based relaxations of the optimal power flow problem," *IEEE Transactions on Power Systems*, vol. 30, no. 6, pp. 3168–3180, 2014.

[17] B. Kocuk, S. S. Dey, and X. A. Sun, "Matrix minor reformulation and SOCP-based spatial branch-and-cut method for the AC optimal power flow problem," *Mathematical Programming Computation*, vol. 10, no. 4, pp. 557–596, 2018.

[18] B. Kocuk, S. Dey, and X. Sun, "Strong SOCP relaxations for the optimal power flow problem," *Operations Research*, vol. 64, no. 6, pp. 1177–1196, 2016.

[19] F. Zohrizadeh, C. Josz, M. Jin, R. Madani, J. Lavaei, and S. Sojoudi, "Conic relaxations of power system optimization: Theory and algorithms," *European Journal of Operational Research*, vol. 287, no. 2, 2020.

[20] O. Alsac and B. Stott, "Optimal load flow with steady-state security," *IEEE Transactions on Power Apparatus and Systems*, vol. 93, no. 3, pp. 745 – 751, 1974.

[21] A. Monticelli, M. V. F. Pereira, and S. Granville, "Security-constrained optimal power flow with post-contingency corrective rescheduling," *IEEE Transactions on Power Systems*, vol. 2, no. 1, pp. 175–180, 1987.

[22] F. Capitanescu, J. Martinez Ramos, P. Panciatici, D. Kirschen, A. Marano Marcolini, L. Platbrood, and L. Wehenkel, "State-of-the-art, challenges, and future trends in security constrained optimal power flow," *Electric Power Systems Research*, vol. 81, no. 8, pp. 1731 – 1741, 2011.

[23] F. Capitanescu, M. Glavic, D. Ernst, and L. Wehenkel, "Contingency filtering techniques for preventive security-constrained optimal power flow," *IEEE Transactions on Power Systems*, vol. 22, no. 4, pp. 1690–1697, 2007.

[24] F. Bouffard, F. Galiana, and J. Arroyo, "Umbrella contingencies in security-constrained optimal power flow," in *Proc. of the 15th Power Systems Computation Conference (PSCC)*, 2005.

[25] R. Madani, J. Lavaei, and R. Baldick, "Constraint screening for security analysis of power networks," *IEEE Transactions on Power Systems*, vol. 32, no. 3, pp. 1828–1838, 2017.

[26] Y. Li and J. D. McCalley, "Decomposed SCOPF for improving efficiency," *IEEE Transactions on Power Systems*, vol. 24, no. 1, pp. 494–495, 2009.

[27] A. Marano-Marcolini, F. Capitanescu, J. L. Martinez-Ramos, and L. Wehenkel, "Exploiting the use of DC SCOPF approximation to improve iterative AC SCOPF algorithms," *IEEE Transactions on Power Systems*, vol. 27, no. 3, pp. 1459–1466, 2012.

[28] Q. Wang, J. D. McCalley, T. Zheng, and E. Litvinov, "Solving corrective risk-based security-constrained optimal power flow with Lagrangian relaxation and Benders decomposition," *International Journal of Electrical Power & Energy Systems*, vol. 75, pp. 255–264, 2016.

[29] K. Karoui, H. Crisciu, A. Szekut, and M. Stubbe, "Large scale security constrained optimal power flow," in *Proc. of the 16th Power Systems Computation Conference (PSCC)*, 2008.

[30] M. Bazrafshan, K. Baker, and J. Mohammadi, "Computationally efficient solutions for large-scale security-constrained optimal power flow," *arXiv preprint https://arxiv.org/pdf/2006.00585.pdf*, 2020.

[31] I. Avramidis, F. Capitanescu, S. Karagiannopoulos, and E. Vrettos, "A novel approximation of security-constrained optimal power flow with incorporation of generator frequency and voltage control response," *IEEE Transactions on Power Systems*, 2020.

[32] J. Mohammadi, G. Hug, and S. Kar, "Agent-based distributed security constrained optimal power flow," *IEEE Transactions on Smart Grid*, vol. 9, no. 2, pp. 1118–1130, 2018.

[33] W. Zhang, Y. Xu, Z. Dong, and K. P. Wong, "Robust security constrained-optimal power flow using multiple microgrids for corrective control of power systems under uncertainty," *IEEE Transactions on Industrial Informatics*, vol. 13, no. 4, pp. 1704–1713, 2017.

[34] E. Karangelos and L. Wehenkel, "An iterative AC-SCOPF approach managing the contingency and corrective control failure uncertainties with a probabilistic guarantee," *IEEE Transactions on Power Systems*, vol. 34, no. 5, pp. 3780–3790, 2019.

[35] A. Velloso and P. Van Hentenryck, "Combining deep learning and optimization for preventive security-constrained DC optimal power flow," *IEEE Transactions on Power Systems*, 2021.

[36] F. Capitanescu, T. V. Cutsem, and L. Wehenkel, "Coupling optimization and dynamic simulation for preventive-corrective control of voltage instability," *IEEE Transactions on Power Systems*, vol. 24, no. 2, pp. 796–805, 2009.

[37] Y. Xu, Z. Y. Dong, R. Zhang, K. P. Wong, and M. Lai, "Solving preventive-corrective SCOPF by a hybrid computational strategy," *IEEE Transactions on Power Systems*, vol. 29, no. 3, pp. 1345–1355, 2014.

[38] D. Zigic, L. T. Watson, E. G. Collins, and D. S. Bernstein, "Homotopy approaches to the H_2 reduced order model problem," 1991.

[39] H. Feng and J. Lavaei, "Damping with varying regularization in optimal decentralized control," 2019, available online at https://lavaei.ieor.berkeley.edu/ODC_hom_2019_2.pdf.

[40] P. Garrigues and L. E. Ghaoui, "An homotopy algorithm for the lasso with online observations," in *Advances in Neural Information Processing Systems*, 2009, pp. 489–496.

[41] L. T. Watson and R. T. Haftka, "Modern homotopy methods in optimization," *Computer Methods in Applied Mechanics and Engineering*, vol. 74, no. 3, pp. 289–305, September 1989.

[42] A. Poore and Q. Al-Hassan, "The expanded Lagrangian system for constrained optimization problems," *SIAM Journal on Control and Optimization*, vol. 26, no. 2, p. 417–427, 1988.

[43] D. M. Dunlavy and D. P. O'Leary, "Homotopy optimization methods for global optimization," *Sandia National Laboratories Report*, December 2005.

[44] H. Mobahi and J. W. Fisher III, "A theoretical analysis of optimization by Gaussian continuation," *AAAI Conference on Artificial Intelligence, North America*, February 2015.

[45] H.-D. Chiang, T.-Q. Zhao, J.-J. Deng, and K. Koyanagi, "Homotopy-enhanced power flow methods for general distribution networks with distributed generators," *IEEE Transactions on Power Systems*, vol. 29, no. 1, pp. 93–100, January 2014.

[46] A. Pandey, M. Jereminov, M. Wagner, G. Hug, and L. Pileggi, "Robust convergence of power flow using Tx stepping method with equivalent circuit formulation," November 2017.

[47] S. Yu, H. D. Nguyen, and K. S. Turitsyn, "Simple certificate of solvability of power flow equations for distribution systems," *2015 IEEE Power & Energy Society General Meeting*, July 2015.

[48] D. Mehta, H. D. Nguyen, and K. Turitsyn, "Numerical polynomial homotopy continuation method to locate all the power flow solutions," *IET Generation, Transmission & Distribution*, vol. 10, no. 12, pp. 2972 – 2980, August 2016.

[49] V. Ajjarapu and C. Christy, "The continuation power flow: A tool for steady state voltage stability analysis," *IEEE Transactions on Power Systems*, vol. 7, no. 1, pp. 416–423, February 1992.

[50] D. P. Bertsekas, *Nonlinear programming*. Athena scientific, 2016.

[51] V. H. Hinojosa and F. Gonzalez-Longatt, "Preventive security-constrained DCOPF formulation using power transmission distribution factors and line outage distribution factors," *Energies*, vol. 11, no. 6, 2018.

[52] J. E. Spingarn, "Multifunctions and integrands." Springer, 1984, ch. Multifunctions associated with parametrized classes of constrained optimization problems, pp. 206–215.

[53] J. Guddat, F. Vasquez, and H.Th.Jongen, *Parametric optimization: singularities, pathfollowing and jumps*. Springer, 1990.

[54] A. Nemirovski, "Interior point polynomial time methods in convex programming," lecture notes from Georgia Tech.

[55] J. E. Spingarn, "Fixed and variable constraints in sensitivity analysis," *SIAM Journal Control and Optimization*, vol. 18, pp. 297–310, 1980.

[56] L. A. Clarfeld, P. D. H. Hines, E. M. Hernandez, and M. J. Eppstein, "Risk of cascading blackouts given correlated component outages," *IEEE Transactions on Network Science and Engineering*, vol. 7, no. 3, pp. 1133–1144, 2020.

[57] Vaiman, Bell, Chen, Chowdhury, Dobson, Hines, Papic, Miller, and Zhang, "Risk assessment of cascading outages: Methodologies and challenges," *IEEE Transactions on Power Systems*, vol. 27, no. 2, pp. 631–641, 2012.

[58] R. D. Zimmerman, C. E. Murillo-Sanchez, and R. J. Thomas, "MATPOWER: Steady-state operations, planning and analysis tools for power systems research and education," *IEEE Transactions on Power Systems*, vol. 26, no. 1, pp. 12–19, February 2011.

[59] H. Wang, C. E. Murillo-Sánchez, R. D. Zimmerman, and R. J. Thomas, "On computational issues of market-based optimal power flow," *IEEE Transactions on Power Systems*, vol. 22, no. 3, pp. 1185–1193, August 2007.

[60] C. Josz, S. Fliscounakis, J. Maeght, and P. Panciatic, "AC power flow data in MATPOWER and QCQP format: iTesla, RTE snapshots, and PEGASE," available online at http://arxiv.org/abs/1603.01533.

[61] S. Fliscounakis, P. Panciatici, F. Capitanescu, and L. Wehenkel, "Contingency ranking with respect to overloads in very large power systems taking into account uncertainty, preventive and corrective actions," *IEEE Transactions on Power Systems*, vol. 28, no. 4, pp. 4909 – 4917, November 2013.

[62] A. V. Fiacco, "Sensitivity analysis for nonlinear programming using penalty methods," *Mathematical Programming*, vol. 10, pp. 287–311, 1976.

[63] D. Kirschen, R. Allan, and G. Strbac, "Contributions of individual generators to loads and flows," *IEEE Transactions on Power Systems*, vol. 12, no. 1, pp. 52–60, Feburary 1997.

8. Appendix

8.1. Proof of Theorem 1

Due to the continuity of $\lambda(t)$, we can equivalently prove that a sufficiently small $\Delta\lambda$ will ensure the desired result, where $\Delta\lambda := \sup_{i=1,\ldots,T-1}(\Lambda^{i+1} - \Lambda^i)$. Let x_1^* denote the unique global solution satisfying SSOC for the problem H_{Λ^1}. Using an argument relying on the implicit function theorem [62], it follows that for each (x_1^*, Λ^1) pair, there exist a neighborhood $\mathbb{U}_1$ around Λ^1 and a neighborhood $\mathbb{X}_1$ around x_1^*, and there is a differentiable function $x_1(\lambda)$ defined for $\lambda \in \mathbb{U}_1$ such that

1. $x_1(\Lambda^1) = x_1^*$
2. For each $\lambda \in \mathbb{U}_1$, $x_1(\lambda)$ is the unique point in $\mathbb{X}_1$ satisfying the SSOC for H_λ.

Now, suppose that $\Delta\lambda$ is small enough so that $\Lambda^2 \in \mathbb{U}_1$. Then, since $x_1(\lambda)$ is a continuous function and there is no λ on the path $\lambda(t) = 0$ such that H_λ has more than one global minimizer, $x_1(\Lambda^2)$ becomes the unique global minimizer satisfying SSOC for the next OPF problem, H_{Λ^2}. The same logic can be applied for all Λ^i, and by induction we have proved the result. ∎

8.2. Proof of Theorem 2

We begin by defining the radius of convergence for Wilson's method for solving H_t in a neighborhood of a local minimizer $w(t)$.

DEFINITION 1.

$$r(t, w(t)) = \sup\{r \mid \text{for all } w^0 \text{ satisfying } \|w^0 - w(t)\| \leq r, \text{ starting Wilson's method with } w^0$$
$$\text{provides a sequence } \{w^i\} \text{ converging to } w(t)\}. \tag{17}$$

The following lemma is a natural corollary of Theorem 3.2.1 in [53]. We do not state the proof of this lemma here but the derivation uses properties of the Wilson's method.

LEMMA 5. *Suppose that Assumptions* $(A1), (A2)$ *and* $(A3)$ *hold. Then, there exists a real number* $\hat{r} > 0$ *such that*

$$r(t, w(t)) \geq \hat{r} \text{ for all } w(t), \ t \in [0,1] \tag{18}$$

Let us consider the sequence $\{w_i'\}_{i=1}^T$ such that

$$\|w_1' - w^*(t^1)\| < \epsilon, \tag{19}$$

$$\|w_i' - \hat{w}^M(w_{i-1}', t)\| < \epsilon', \quad i = 2, \ldots, T, \tag{20}$$

where $0 < \epsilon' \ll \epsilon$ and $\hat{w}^M(w_k', t)$ denotes the true (or exact) KKT point after applying M Wilson's steps starting from w_k'. The choice of w_1' satisfying (19) is possible because of the known initial global minimizer assumption in (A_1). From the proof of Theorem 3.2.1 in [53], we also know that

there is a constant $\hat{r} > 0$ such that $\|\hat{w}(w, t) - w^*(t^i)\| \leq \frac{1}{2}\|w - w^*(t^i)\|$ whenever $\|w - w^*(t^i)\| \leq \hat{r}$. Now, we choose $\epsilon > 0$ and $\eta > 0$ such that the following condition is satisfied:

$$\epsilon + \eta < \hat{r} \tag{21}$$

Due to the assumption on the continuity of the global minimizers (A_1), there is a $\Delta t > 0$ such that

$$\|w^*(\tilde{t}) - w^*(t)\| < \eta, \quad \text{for all } \tilde{t}, t \in [0, 1] \text{ with } \|\tilde{t} - t\| \leq \Delta t \tag{22}$$

Given t^k and w'_k with $\|w'_k - w^*(t^k)\| < \epsilon$ for some $k \in \{1, \ldots, T-1\}$, we obtain

$$\|w'_k - w^*(t^{k+1})\| \leq \|w'_k - w^*(t^k)\| + \|w^*(t^k) - w^*(t^{k+1})\| < \epsilon + \eta < \hat{r} \tag{23}$$

Hence, the point w'_k is in the region of convergence and therefore,

$$\|\hat{w}^M(w'_k, t) - w^*(t^{k+1})\| \leq \left(\frac{1}{2}\right)^M (\epsilon + \eta) \tag{24}$$

Furthermore, we obtain

$$\|w'_{k+1} - w^*(t^{k+1})\| \leq \|w'_{k+1} - \hat{w}^M(w'_k, t)\| + \|\hat{w}^M(w'_k, t) - w^*(t^{k+1})\| \leq \epsilon' + \left(\frac{1}{2}\right)^M (\epsilon + \eta) \tag{25}$$

To find M, we need to ensure that the equation (25) can be upper bounded by ϵ:

$$\epsilon' + \left(\frac{1}{2}\right)^M (\epsilon + \eta) \leq \epsilon \tag{26}$$

Solving for M, we obtain the condition

$$M \geq \log_2 \frac{\epsilon + \eta}{\epsilon - \epsilon'} \tag{27}$$

Noting that $\hat{r} > \epsilon + \eta$ from equation (21) and $\epsilon' \ll \epsilon$, we observe that M satisfies the condition (27) if $M \geq \log_2 \frac{\hat{r}}{\epsilon}$. We can continue this logic until $k = T - 1$ and arrive at the conclusion that the number of Wilson's method that will enable the algorithm to keep track of the global minimizers is on the order of $O(\log(\hat{r}/\epsilon)) \cdot \frac{1}{\Delta t}$. Finally, we claim that $1/\Delta t$ is upper bounded by a constant for sufficiently small ϵ. This is because Δt only needs to be small enough so that η satisfies equation (21). Therefore, if we have a constant $\overline{\Delta t}$ corresponding to some value $\bar{\eta}$ satisfying the condition for a given $\bar{\epsilon}$, the same $\overline{\Delta t}$ (and equivalently $\bar{\eta}$) will satisfy the condition for any ϵ smaller than $\bar{\epsilon}$. This concludes that the overall complexity of solving homotopy-OPF is $O(\log(\hat{r}/\epsilon))$, which is equivalent to $O(\log(1/\epsilon))$ ∎

8.3. Proof of Lemma 1

By Proposition 4 of [52], the family of optimization problems

$$\min_{x \in \Psi} \quad \bar{f}(x, \lambda, \omega)$$
$$\text{s.t.} \quad h(x, \lambda) = 0$$

has a unique global minimizer satisfying SSOC for all parameters $(\lambda, \omega) \in \mathbb{U}$ except on a set of measure zero if (i) for all $x_1 \neq x_2$, and for all ω, the function $\omega \to \bar{f}(x_1, \lambda, \omega) - \bar{f}(x_2, \lambda, \omega)$ is of rank one at all λ, (ii) the function $\lambda \to h(x, \lambda)$ is of full rank $2|\mathcal{V}|$ for all x at every ω, and (iii) the fixed set Ψ is a cyrtohedron and $\mathbb{U}$ is an open set. It is straightforward to check that if $\bar{f}(x, \lambda, \omega) = f(x, \lambda) + \omega^T x$, condition (i) is satisfied. Conditions (ii) and (iii) are given as assumptions, which completes the proof. ∎

8.4. Proof of Lemma 2

The rank of the function $\lambda \to h(x, \lambda)$ is the rank of its Jacobian (w.r.t. λ). Therefore, we analyze the Jacobian of $h(x, \lambda) = h(x, [\gamma, \beta, \gamma^{\text{sh}}, \beta^{\text{sh}}])$ with respect to $[\gamma, \beta, \gamma^{\text{sh}}, \beta^{\text{sh}}]$. From Section 3.2 and 4.1, we know that h consists of two types of functions, h^1 and h^2 (corresponding to the real power flow equations and the reactive power flow equations, respectively), whose i-th elements are defined by:

$$h_i^1(x, [\gamma, \beta, \gamma^{\text{sh}}, \beta^{\text{sh}}]) = P_i^g - P_i^d - \sigma_i^p - \sum_{j \in \mathcal{N}(i)} \frac{g_{ij}^{\text{sh}} \gamma_{ij}^{\text{sh}}}{2} |v_i|^2$$
$$- \sum_{j \in \mathcal{N}(i)} g_{ij} \gamma_{ij} (|v_i|^2 - |v_i||v_j| \cos \theta_{ij}) - b_{ij} \beta_{ij} |v_i||v_j| \sin \theta_{ij}$$

$$h_i^2(x, [\gamma, \beta, \gamma^{\text{sh}}, \beta^{\text{sh}}]) = q_i^g - Q_i^d - \sigma_i^q + \sum_{j \in \mathcal{N}(i)} \frac{b_{ij}^{\text{sh}} \beta_{ij}^{\text{sh}}}{2} |v_i|^2$$
$$+ \sum_{j \in \mathcal{N}(i)} b_{ij} \beta_{ij} (|v_i|^2 - |v_i||v_j| \cos \theta_{ij}) - g_{ij} \gamma_{ij} |v_i||v_j| \sin \theta_{ij}$$

We focus on the submatrix of the Jacobian that consists only of the derivatives of h_i^1 and h_i^2 with respect to γ^{sh} and β^{sh} (denote this as J). This is because if this submatrix has full column rank, then the full Jacobian also has full column rank. First, we notice that the Jacobian of h^1 with respect to β^{sh} and the Jacobian of h^2 with respect to γ^{sh} are equal to zero. Therefore, J can be expressed as a 2×2 block matrix of the form $J = \left[\begin{array}{c|c} J^1 & 0 \\ \hline 0 & J^2 \end{array} \right] \in \mathbb{R}^{2|\mathcal{E}| \times 2|\mathcal{V}|}$, where J^1 corresponds to the Jacobian of h^1 with respect to γ^{sh} and J^2 corresponds to the Jacobian of h^2 with respect to β^{sh}.

For line outage contingencies, γ^{sh} and β^{sh} are parameters indexed by the line number. Hereby, let $J^1_{((i,j),k)}$ refer to the element of J^1 that is located at the (i,j)-th row and the k-th column (the

row index representing the line and the column index representing the bus number). For example, $J^1_{((i,j),k)}$ denotes the partial derivative of the real power flow equation at bus k with respect to the shunt susceptance parameter at line (i,j). The same goes for J^2.

Then, directly from basic calculus, we can derive the following form for the matrix J:

$$J^1_{(i,j),k} = \begin{cases} -\frac{1}{2}g^{\text{sh}}_{ij}|v_k|^2 & \text{for } k = i \text{ or } j, \ j \in \mathcal{N}(i) \\ 0 & \text{otherwise} \end{cases}$$

$$J^2_{(i,j),k} = \begin{cases} \frac{1}{2}b^{\text{sh}}_{ij}|v_k|^2 & \text{for } k = i \text{ or } j, \ j \in \mathcal{N}(i) \\ 0 & \text{otherwise} \end{cases}$$

Therefore, if J has full column rank, so will the Jacobian of the function $\lambda \to h(x,\lambda)$, which completes the proof. ∎

8.5. Proof of Lemma 3

Similar to the proof of Lemma 2, we analyze the Jacobian of $h(x,\lambda) = h(x,[\gamma,\beta])$ with respect to $[\gamma,\beta]$. From Section 3.2 and 4.1, we know that h consists of two types of functions, h^1 and h^2 (corresponding to the real power flow equations and the reactive power flow equations, respectively), whose i-th elements are defined by:

$$\begin{aligned} h^1_i(x,[\gamma,\beta]) = \ & P^{g,o}_i \gamma_i + P^{g,f}_i(1-\gamma_i) - P^d_i - \sigma^p_i \\ & - \sum_{j \in \mathcal{N}(i)} g_{ij}\gamma_{ij}(|v_i|^2 - |v_i||v_j|\cos\theta_{ij}) - b_{ij}\beta_{ij}|v_i||v_j|\sin\theta_{ij} \\ & - \sum_{j \in \mathcal{N}(i)} \frac{g^{\text{sh}}_{ij}\gamma^{\text{sh}}_{ij}}{2}|v_i|^2 \end{aligned}$$

$$\begin{aligned} h^2_i(x,[\gamma,\beta]) = \ & q^g_i - Q^{d,o}_i\beta_i - Q^{d,f}_i(1-\beta_i) - \sigma^q_i \\ & + \sum_{j \in \mathcal{N}(i)} b_{ij}\beta_{ij}(|v_i|^2 - |v_i||v_j|\cos\theta_{ij}) - g_{ij}\gamma_{ij}|v_i||v_j|\sin\theta_{ij} \\ & + \sum_{j \in \mathcal{N}(i)} \frac{b^{\text{sh}}_{ij}\beta^{\text{sh}}_{ij}}{2}|v_i|^2 \end{aligned}$$

First, we notice that the Jacobian of h^1 with respect to β and the Jacobian of h^2 with respect to γ are equal to zero. Therefore, M can be expressed as a 2×2 block matrix of the form $M = \begin{bmatrix} M^1 & 0 \\ 0 & M^2 \end{bmatrix} \in \mathbb{R}^{2|\mathcal{V}| \times 2|\mathcal{V}|}$ where M^1 corresponds to the Jacobian of h^1 with respect to γ and M^2 corresponds to the Jacobian of h^2 with respect to β.

For generator outage contingencies, γ and β are parameters indexed by the bus number (because we assume each bus has exactly one generator). Hereby, let $M^1_{i,j}$ refer to the element of M^1 that is located at the i-th row and the j-th column. In other words, $M^1_{i,j}$ denotes the partial derivative of

the real power flow equation at bus i with respect to the γ parameter at bus j. The same goes for M^2.

Then, directly from basic calculus, we can derive the following form for the matrix M:

$$M^1_{i,j} = \begin{cases} P^{g,o}_i - P^{g,f}_i & \text{for } j = i \\ 0 & \text{otherwise} \end{cases}$$

$$M^2_{i,j} = \begin{cases} Q^{d,o}_i - Q^{d,f}_i & \text{for } j = i \\ 0 & \text{otherwise} \end{cases}$$

Therefore, if M has full column rank, so will the Jacobian of the function $\lambda \to h(x, \lambda)$, which completes the proof. ∎

8.6. Proof of Corollary 1

The first statement on $H_{\lambda,\omega}$ having a unique global minimizer satisfying SSOC follows directly from applying Lemma 1. The functions $\lambda \to h(x, \lambda)$ is of full rank $2|\mathcal{V}|$ due to Lemmas 2 and 3, and this in turn satisfies the first condition of Lemma 1. As discussed in Section 5, the set Ψ is a cyrtohedron, and the set $\mathbb{U}$ is defined to be an open set for any $\epsilon > 0$ by the assumptions of this theorem. In other words, the second condition of Lemma 1 is also satisfied. Therefore, we can conclude that for any value of $\epsilon > 0$, $H_{\lambda,\omega}$ has a unique global minimizer satisfying SSOC for every $(\lambda, \omega) \in \mathbb{U} \setminus \mathbb{U}'$ where $\mathbb{U}' \subset \mathbb{U}$ is of measure zero.

8.7. Proof of Lemma 4

Let us start with the equation for the reactive power injections. Let θ_1 and θ_2 denote the voltage phasor angles at buses 1 and 2, respectively. Let the real and reactive power injections at bus i be denoted by p^{inj}_i and q^{inj}_i, respectively. In this two-bus example, we consider the objective function: $(\sigma^p_1)^2 + c(\sigma^p_2)^2$. Then after denoting $\theta = \theta_1 - \theta_2$, we have the following:

$$q^{\text{inj}}_1 = B\beta - G\gamma \cdot \sin\theta - B\beta \cdot \cos\theta$$
$$q^{\text{inj}}_2 = B\beta + G\gamma \cdot \sin\theta - B\beta \cdot \cos\theta$$

A lower bound of $Q^{\min}$ on q^{inj}_1 results in the following:

$$Q^{\min} \leq B\beta - G\gamma \cdot \sin\theta - B\beta \cdot \cos\theta$$

Then, after rearranging and using trigonometry, we arrive at

$$-Q^{\min} + B\beta \geq G\gamma \cdot \sin\theta + B\beta \cdot \cos\theta$$
$$= \sqrt{(G\gamma)^2 + (B\beta)^2} \cdot \cos(\theta - \Delta) \quad \text{where } \Delta = \tan^{-1}\left(\frac{G\gamma}{B\beta}\right).$$

After dividing both sides by $\sqrt{(G\gamma)^2 + (B\beta)^2}$, we have

$$\cos(\theta - \Delta) \leq \frac{-Q^{\min} + B\beta}{\sqrt{(G\gamma)^2 + (B\beta)^2}}$$

which implies

$$\theta \geq \cos^{-1}\left(\frac{-Q^{\min} + B\beta}{\sqrt{(G\gamma)^2 + (B\beta)^2}}\right) + \Delta \quad \text{or} \quad \theta \leq -\cos^{-1}\left(\frac{-Q^{\min} + B\beta}{\sqrt{(G\gamma)^2 + (B\beta)^2}}\right) + \Delta \tag{28}$$

From the lower bound on q_2^{inj}, we can perform a similar derivation and arrive at

$$\theta \geq \cos^{-1}\left(\frac{-Q^{\min} + B\beta}{\sqrt{(G\gamma)^2 + (B\beta)^2}}\right) - \Delta \quad \text{or} \quad \theta \leq -\cos^{-1}\left(\frac{-Q^{\min} + B\beta}{\sqrt{(G\gamma)^2 + (B\beta)^2}}\right) - \Delta. \tag{29}$$

Therefore, combining inequalities (28) and (29) leads to

$$\theta \geq \cos^{-1}\left(\frac{-Q^{\min} + B\beta}{\sqrt{(G\gamma)^2 + (B\beta)^2}}\right) + \Delta \quad \text{or} \quad \theta \leq -\cos^{-1}\left(\frac{-Q^{\min} + B\beta}{\sqrt{(G\gamma)^2 + (B\beta)^2}}\right) - \Delta. \tag{30}$$

Furthermore, we assume that

$$-\tan^{-1}\left(\frac{B\beta}{G\gamma}\right) \leq \theta \leq \tan^{-1}\left(\frac{B\beta}{G\gamma}\right)$$

which is equivalent to

$$-\left(\frac{\pi}{2} - \Delta\right) \leq \theta \leq \left(\frac{\pi}{2} - \Delta\right) \tag{31}$$

Combining (30) and (31) and using the definition of α yields the final constraint on θ:

$$\alpha + \Delta \leq \theta \leq \left(\frac{\pi}{2} - \Delta\right) \quad \text{or} \quad -\left(\frac{\pi}{2} - \Delta\right) \leq \theta \leq -\alpha - \Delta. \tag{32}$$

This feasible region of θ is reflected in the feasible region of the real power injections, as shown in the bolded part of the ellipse in Figure 7. As illustrated in the figure, the two red points are real power injections, corresponding to $\theta = \alpha + \Delta$ and $\theta = -\alpha - \Delta$. Let the first red point, $(p_1^{\mathrm{inj}}, p_2^{\mathrm{inj}})$, be generated by $\theta = \alpha + \Delta$. Then, one can write:

$$
\begin{aligned}
p_1^{\mathrm{inj}} &= G\gamma + B\beta \cdot \sin\theta - G\gamma \cdot \cos\theta \\
&= G\gamma + B\beta \cdot \sin(\alpha + \Delta) - G\gamma \cdot \cos(\alpha + \Delta) \\
&= G\gamma + B\beta \cdot (\sin\alpha \cdot \cos\Delta + \alpha\sin\Delta) - G\gamma \cdot (\alpha\cos\Delta - \sin\alpha \cdot \sin\Delta) \\
&= G\gamma + \frac{B\beta}{|y|}(B\beta \cdot \sin\alpha + \alpha \cdot G\gamma) - \frac{G\gamma}{|y|}(\alpha \cdot B\beta - G\gamma \cdot \sin\alpha)
\end{aligned}
$$

Similarly, if we let the second red point $(\bar{p}_1^{\mathrm{inj}}, \bar{p}_2^{\mathrm{inj}})$, be generated by $\theta = -\alpha - \Delta$, we have

$$\bar{p}_1^{\mathrm{inj}} = G\gamma - \frac{B\beta}{|y|}(B\beta \cdot \sin\alpha + \alpha \cdot G\gamma) - \frac{G\gamma}{|y|}(\alpha \cdot B\beta - G\gamma \cdot \sin\alpha)$$
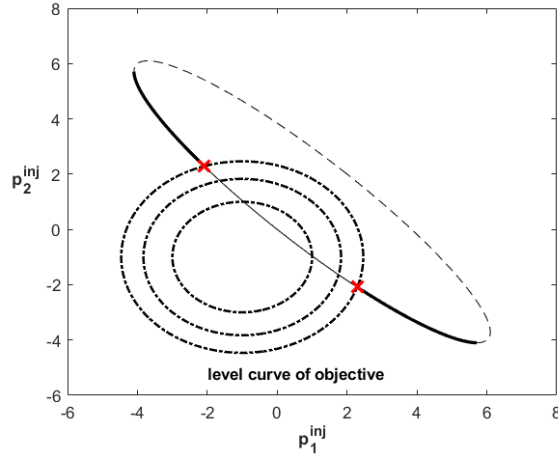
Figure 7 An example of two-bus network for which there are two global solutions to an instance of the homotopy-OPF.

Moreover, note that due to symmetry, $p_2^{\text{inj}} = \bar{p}_1^{\text{inj}}$ and $\bar{p}_2^{\text{inj}} = p_1^{\text{inj}}$. Define the following two functions:

$$\Omega_1(\gamma, \beta) \equiv p_1^{\text{inj}} - \bar{p}_1^{\text{inj}} = \frac{2B\beta}{|y|}\big(B\beta \cdot \sin\alpha + \alpha \cdot G\gamma\big),$$

$$\Omega_2(\gamma, \beta) \equiv p_1^{\text{inj}} + \bar{p}_1^{\text{inj}} = 2G\gamma - \frac{2G\gamma}{|y|}\big(-G\gamma \cdot \sin\alpha + \alpha \cdot B\beta\big).$$

Recall that $P_i^{\text{g,b}}$ denotes the real power generation at bus i obtained from the base-OPF solution. If the two points $(p_1^{\text{inj}}, p_2^{\text{inj}})$ and $(\bar{p}_1^{\text{inj}}, \bar{p}_2^{\text{inj}})$ are both globally optimal, their objective values must be equal. In other words,

$$(p_1^{\text{inj}} - (P_1^{\text{g, b}} - P_1^d))^2 + c(p_2^{\text{inj}} - (P_2^{\text{g, b}} - P_2^d))^2 = (\bar{p}_1^{\text{inj}} - (P_1^{\text{g, b}} - P_1^d))^2 + c(\bar{p}_2^{\text{inj}} - (P_2^{\text{g, b}} - P_2^d))^2.$$

Rearranging the terms leads to

$$(1-c)\{(p_1^{\text{inj}})^2 - (\bar{p}_1^{\text{inj}})^2\} - 2(P_1^{\text{g, b}} - P_1^d)(p_1^{\text{inj}} - \bar{p}_1^{\text{inj}}) + 2c(P_2^{\text{g, b}} - P_2^d)(p_1^{\text{inj}} - \bar{p}_1^{\text{inj}}) = 0$$

Finally, substituting the definition of Ω_1 and Ω_2, we arrive at

$$(1-c) \cdot \Omega_1(\gamma, \beta) \cdot \Omega_2(\gamma, \beta) - 2(P_1^{\text{g, b}} - P_1^d) \cdot \Omega_1(\gamma, \beta) + 2c(P_2^{\text{g, b}} - P_2^d) \cdot \Omega_1(\gamma, \beta) = 0$$

This completes the proof. ∎

8.8. Computation of Participation Factors for Generator Outage

During the outage of one or more generators, a collection of other generators will increase their power generation in order to respond to the outage and meet power demand. The "participation factor" of a generator determines the portion of the generation response that is assigned to that generator. There are a variety of ways to compute participation factors, including scaling the

---

Algorithm 3 Calculation of Participation Factors for Power Redistribution at Contingency k

---

Given: (i) solution to base-OPF problem $(|v|, \theta, p^g, q^g, \{\sigma_k\})$

(ii) generators out in contingency k: $R_k \subset \mathcal{V}$

Compute real power flow for all $(i,j) \in \mathcal{E}$ in the base-case:

$p_{ij} = G_{ij}|v|_i^2 - G_{ij}|v|_i|v|_j \cos(\theta_{ij}) + B_{ij}|v|_i|v|_j \sin(\theta_{ij})$

Generate a directed graph $\mathcal{D}(\mathcal{V}, \mathcal{A})$ based on direction of power flow: $(i,j) \in \mathcal{A}$ if $p_{ij} \geq 0$

Use shortest path algorithm to compute the domain of each generator

Group the buses supplied by the same set of generators into commons $\mathcal{C}$ (see [63])

Use algorithm in [63] to determine the contribution C_{rj} of each generator r to common j

Remove contribution of generators that are out:

$C_{rj} \leftarrow 0 \quad \forall r \in R_k, \;\; \forall j \in \mathcal{C}$

Distribute lost generation over generations that supply the same common:

for $j \in \mathcal{C}$ **do**

    Define $C_j = \sum_r C_{rj}$

    if $C_j \neq 0$ **then**

        for $r \in \mathcal{V}$ **do**

            $C_{rj} \leftarrow C_{rj}/C_j$

        end for

    end if

end for

Initialize participation factors: $\alpha_r^g = 0$ for all $r \in \mathcal{V}$

Define participation factors based on contribution to common:

for $r \in R_k$ **do**

    for $j \in \mathcal{C}$ **do**

        $\alpha_t^g \leftarrow \alpha_t^g + C_{tj}$ for all generators t in common j

    end for

end for

Normalize the participation factors α^g so that $\sum_{r \in \mathcal{V}} \alpha_r^g = 1$

---

participation factors based on the remaining power capacity. In Algorithm 3, we present one method for computing participation factors which is based on the topology of the network, i.e. it redirects generation from the outed generators to generators that supply the same set of buses as the outed generators in the base-OPF. This method is based on the work [63]. In our simulations of generator outages, we use this method for computing participation factors with Algorithm 2.